Supplemental Material for "Statistical properties of inter-event times in seismic time series transformed by occurrence rate: An analysis from the viewpoint of hierarchy in the temporal nature of seismicity"

Hiroki Tanaka[1]

[1]Graduate School of Informatics, Kyoto University, Yoshida-honmachi, Sakyo-ku, Kyoto-shi, 606-8501, Japan

This supplemental material provides the figures for the results related to the main text yet not shown. See the caption of the corresponding figure in the main text for detailed descriptions of the figures. See Sect. 2 of the main text for the seismic catalog information and the preprocessing methods to obtain the time series named CMT, JS, JA, SCA1, SCA2, SCA3, SCS1, and SCS2.

1   Figures S1- for $\Psi_{mM}(i|\tau_M)$, $\Psi_{\Delta m}(i|y)$, and the negative binomial distribution

Figures S1-(1) to S1-(7) show $\Psi_{mM}(i|\tau_M)$, $\Psi_{\Delta m}(i|y)$, and the negative binomial distributions for each time series with Δm values: (a) $\Delta m = 0.5$, (b) $\Delta m = 1.0$, and (c) $\Delta m = 1.5$, for Fig. S1-(1), S1-(3), and S1-(5) – S1-(7); (a) $\Delta m = 0.2$, (b) $\Delta m = 0.4$, (c) $\Delta m = 0.6$, and (d) $\Delta m = 0.8$ for Fig. S1-(2) and S1-(4).
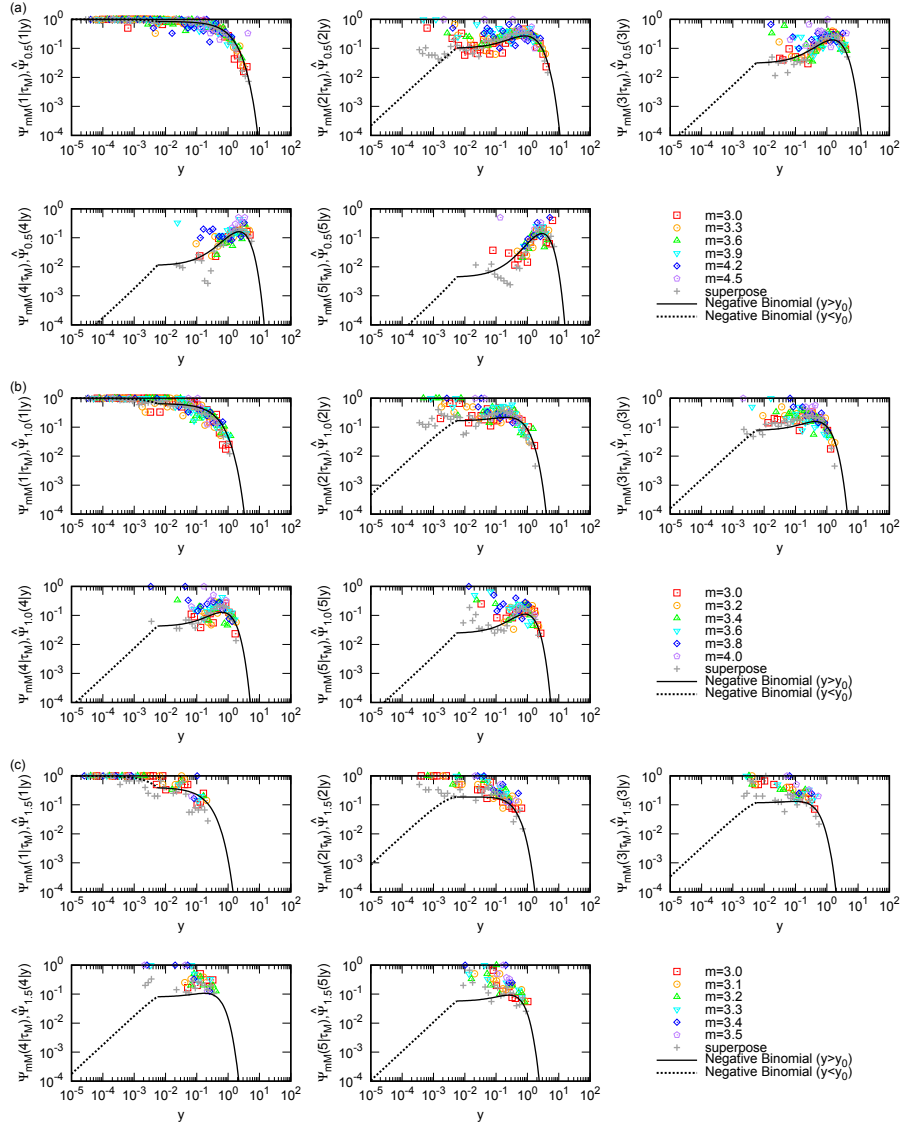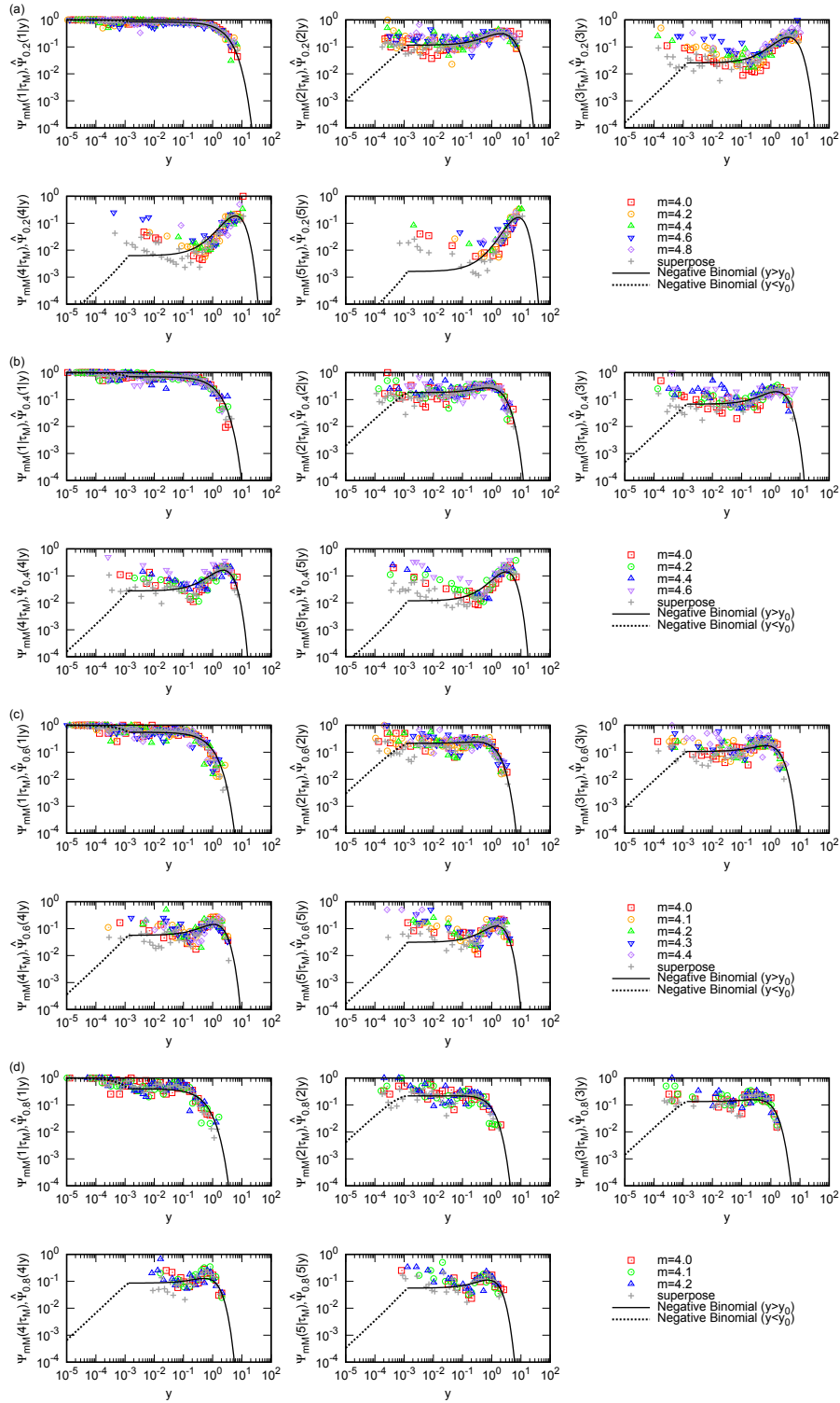
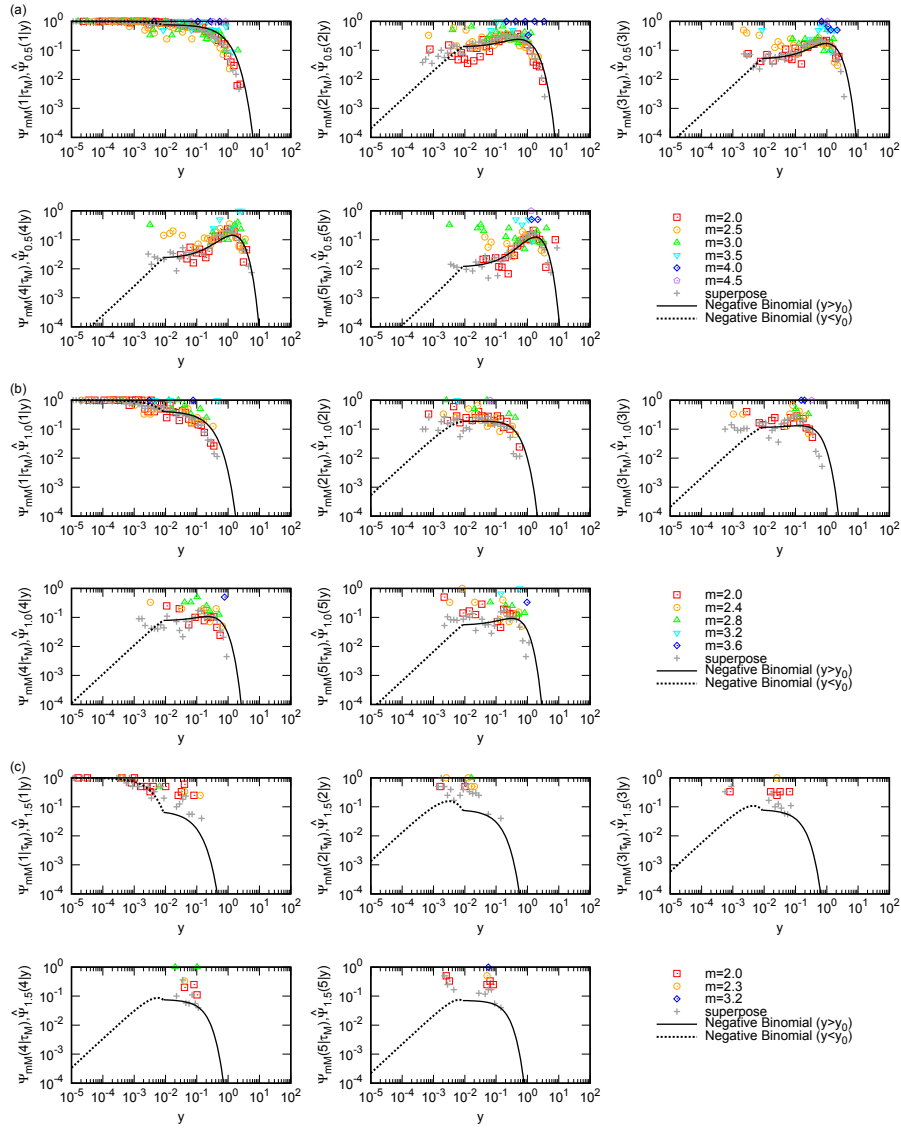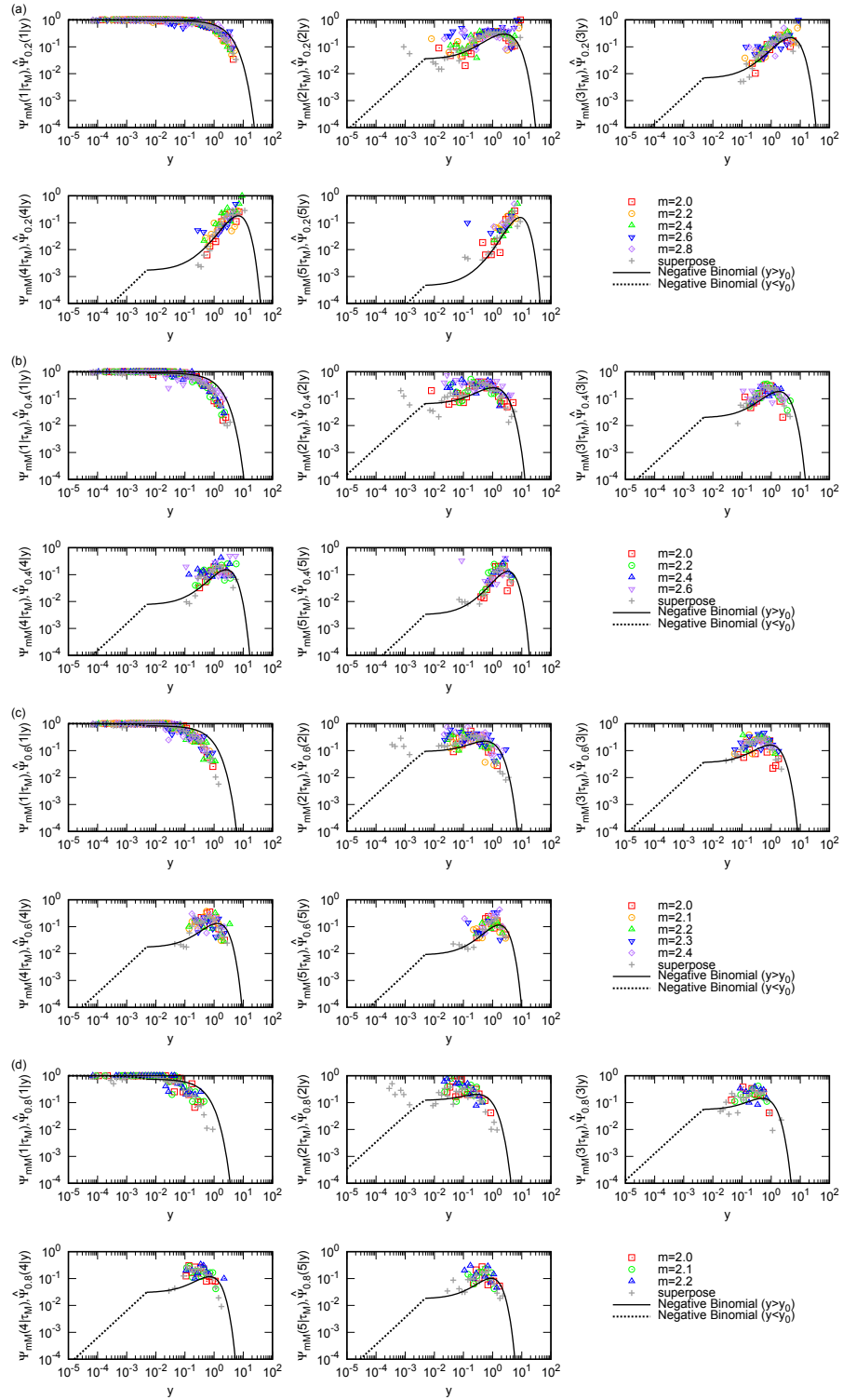Figure S1-(1): JS

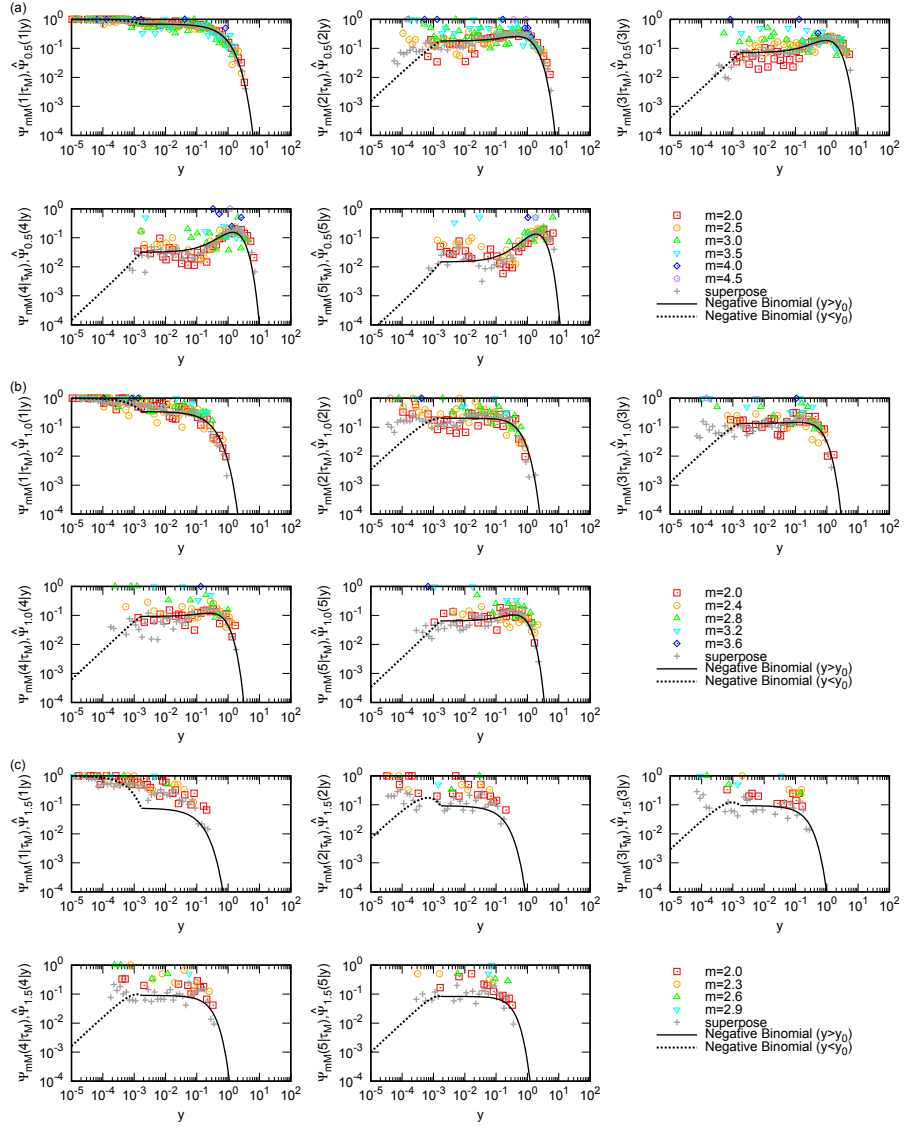Figure S1-(2): JA

3

Figure S1-(3): SCA1
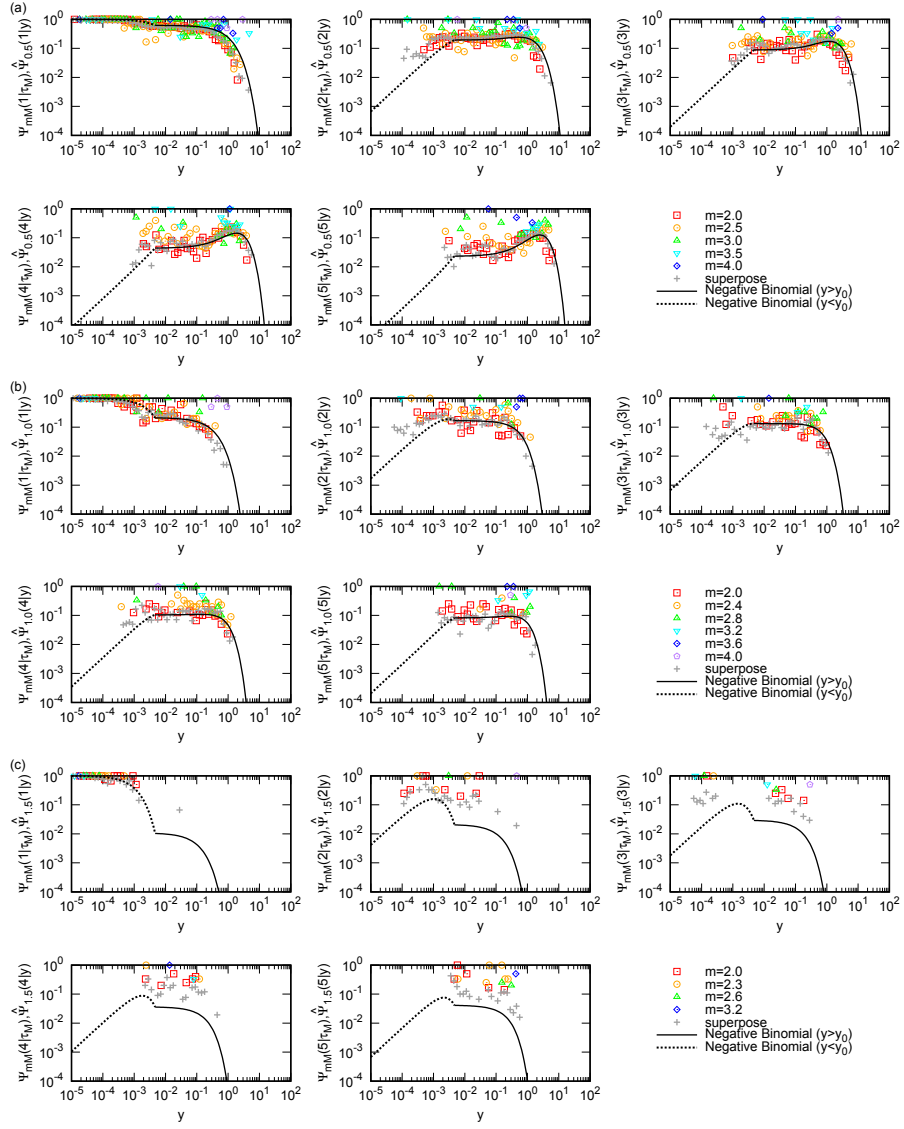
Figure S1-(4): SCA2

Figure S1-(5): SCA3
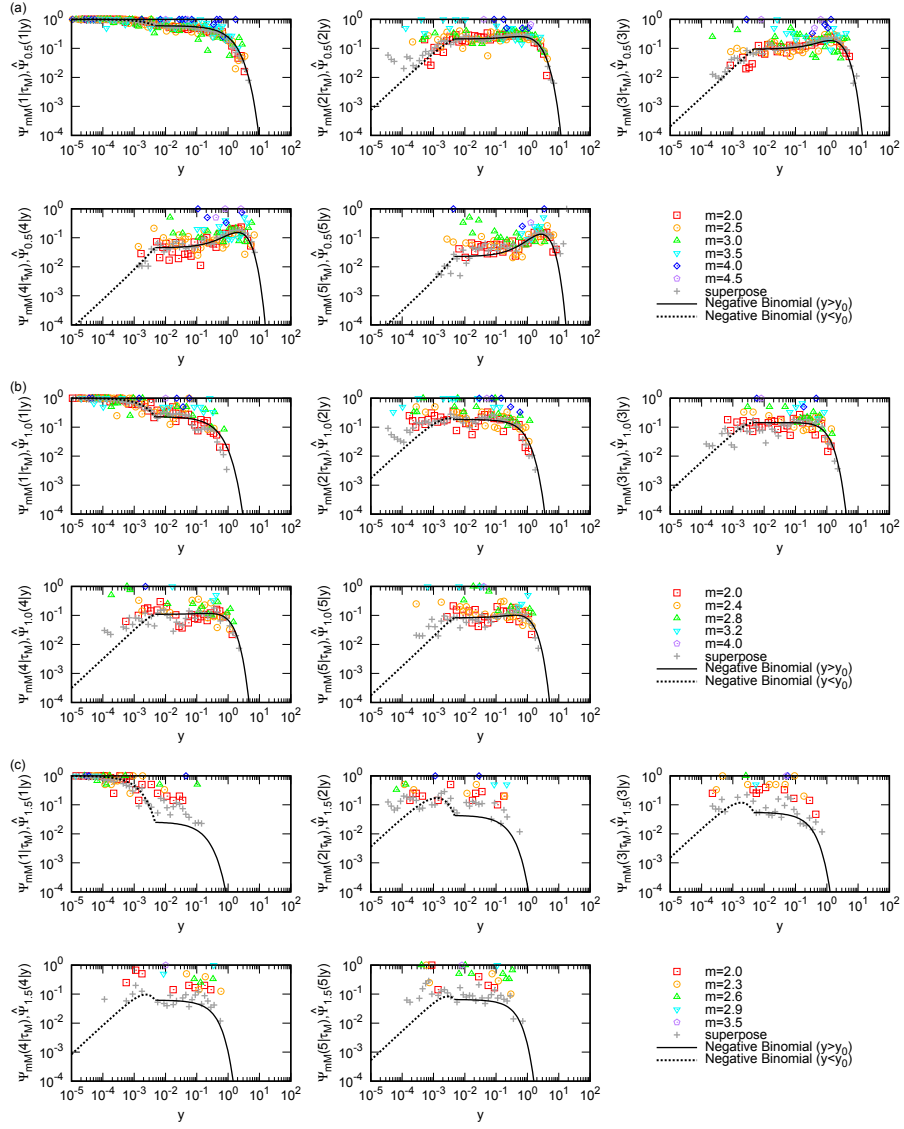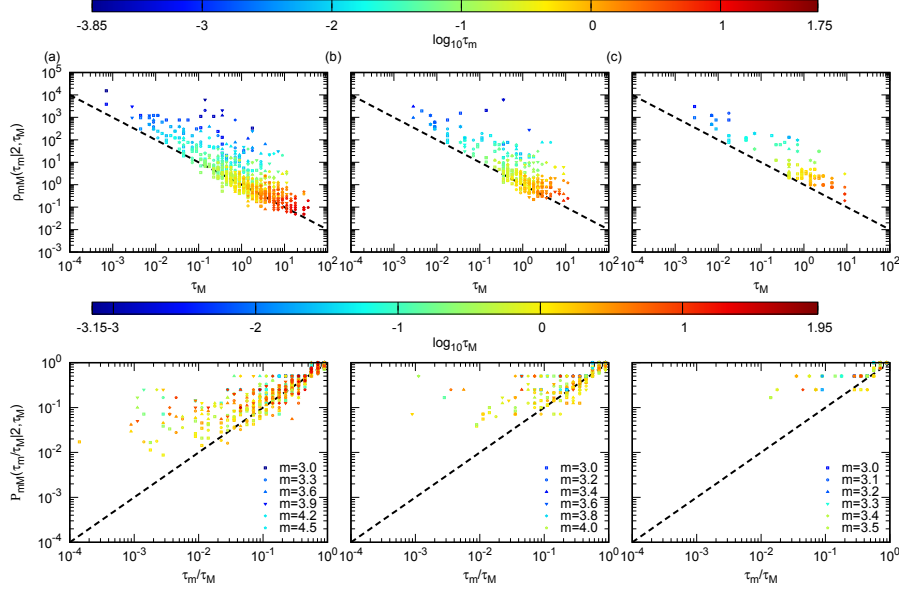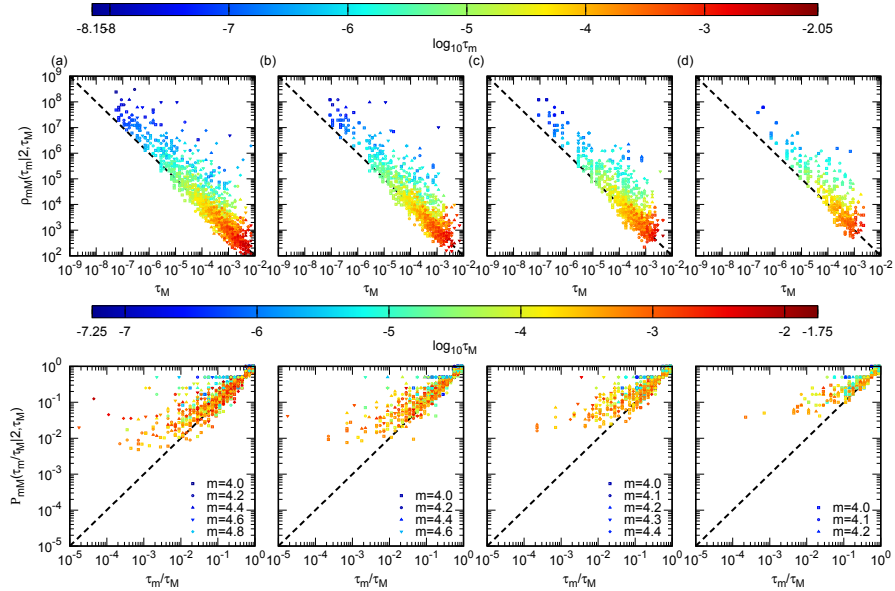
Figure S1-(6): SCS1

Figure S1-(7): SCS2

8

2 Figures S2- for $\rho_{mM}(\tau_m|2, \tau_M)$ and $P_{mM}(\tau_m/\tau_M|2, \tau_M)$

Figures S2-(1) to S2-(7) show $\rho_{mM}(\tau_m|2, \tau_M)$ and $P_{mM}(\tau_m/\tau_M|2, \tau_M)$ for each time series. Δm values are: (a) $\Delta m = 0.5$, (b) $\Delta m = 1.0$, and (c) $\Delta m = 1.5$ for Figs. S2-(1), S2-(3), and S2-(5) – S2-(7); (a) $\Delta m = 0.2$, (b) $\Delta m = 0.4$, (c) $\Delta m = 0.6$, and (d) $\Delta m = 0.8$ for Figs. S2-(2) and S2-(4).

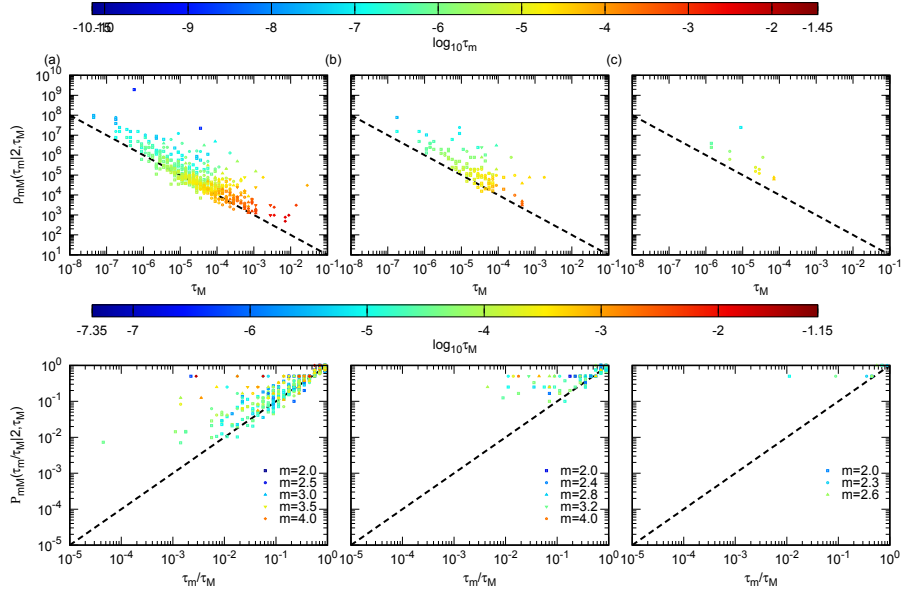

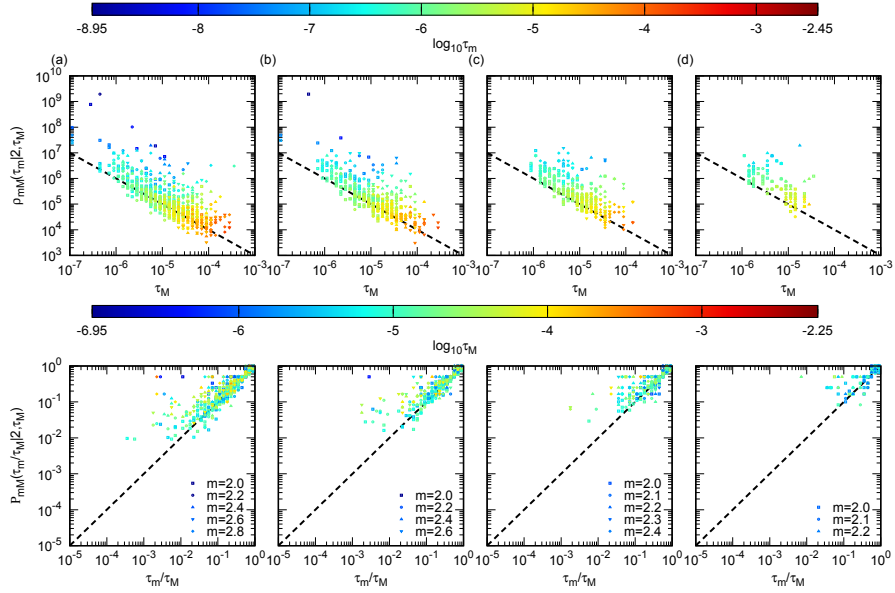Figure S2-(1): JS

Figure S2-(2): JA

Figure S2-(3): SCA1

Figure S2-(4): SCA2
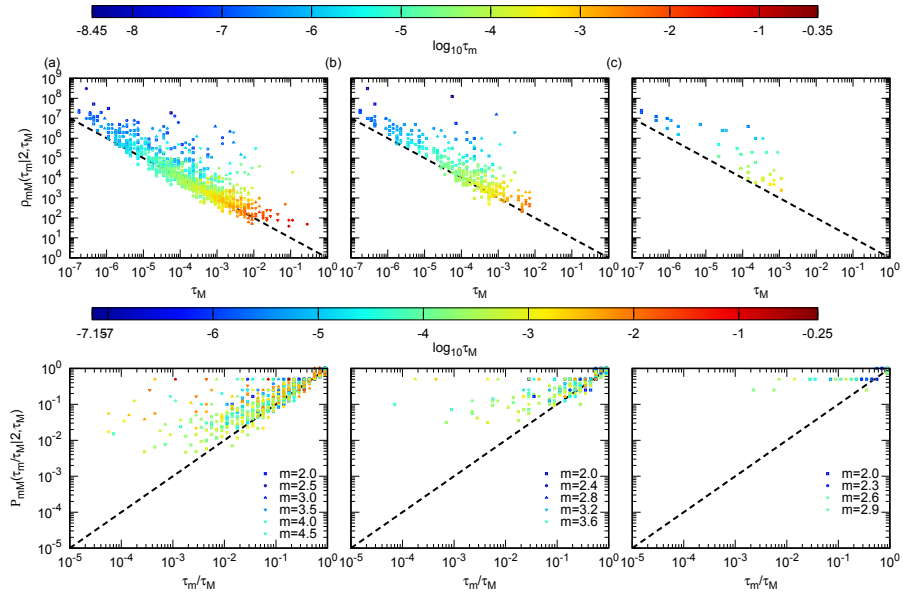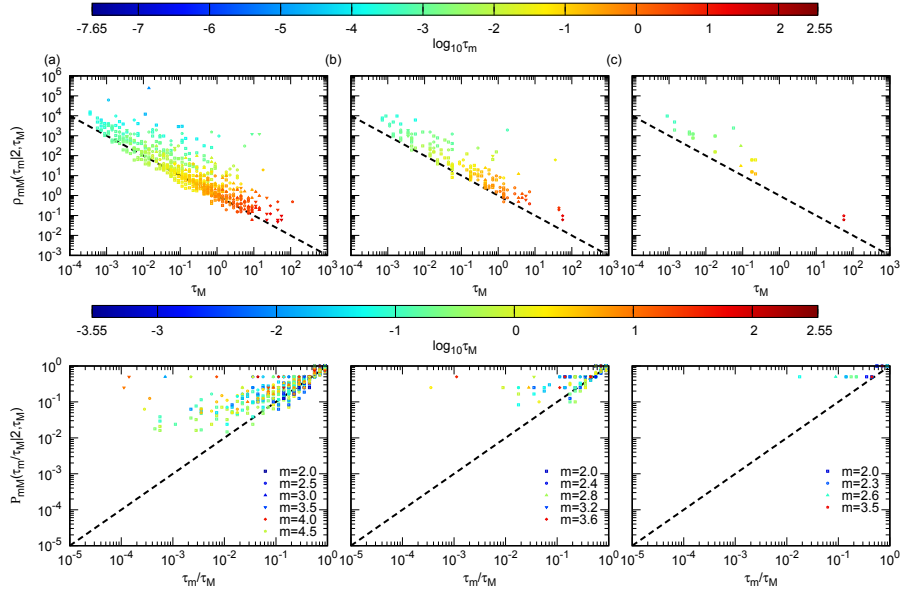
10

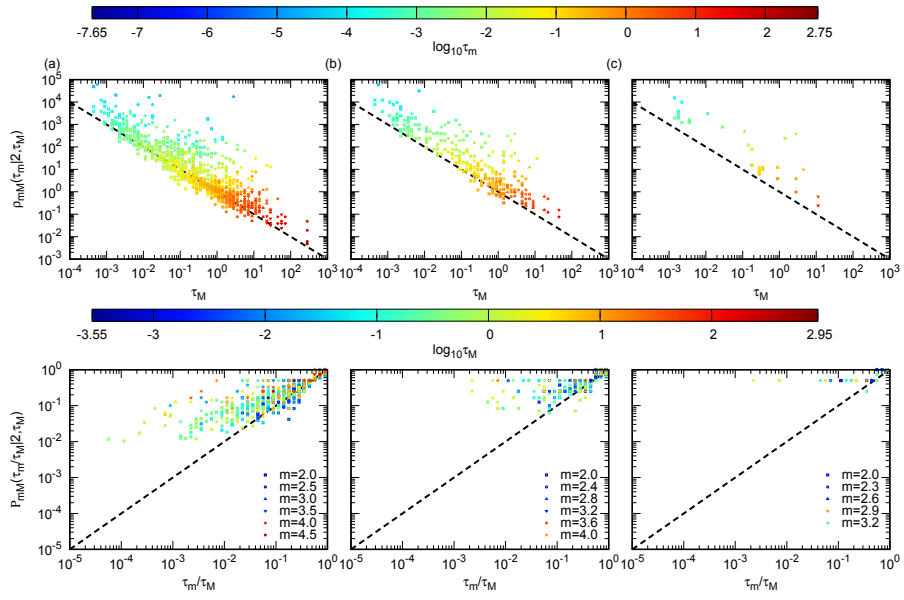Figure S2-(5): SCA3

Figure S2-(6): SCS1

11

Figure S2-(7): SCS2

3 Figures S3- for $\hat{P}_{mM}(x|y)$ and $\overline{P}_{\Delta m}(x|y)$

Figures S3-(1) to S3-(7) show $\hat{P}_{mM}(x|y)$ and $\overline{P}_{\Delta m}(x|y)$ with: (a) $\Delta m = 0.4$, (b) $\Delta m = 0.8$, (c) $\Delta m = 1.2$, and (d) $\Delta m = 1.6$ for Fig. S3-(1); (a) $\Delta m = 0.2$, (b) $\Delta m = 0.4$, (c) $\Delta m = 0.6$, and (d) $\Delta m = 0.8$ for Fig. S3-(2); (a) $\Delta m = 0.6$, (b) $\Delta m = 1.2$, (c) $\Delta m = 1.8$, and (d) $\Delta m = 2.4$ for Figs. S3-(3) – S3-(7). For Figs. S3-(3) – S3-(7), the y ranges to display are chosen from j's such that at least $n_{\min}$ of the (m, M) pairs indicated in the figure's legend fall within the range $(10^{j\Delta\sigma}, 10^{(j+1)\Delta\sigma})$, where $n_{\min}$ is 5 for Figs. S3-(3), S3-(5) – S3-(7) and 4 for Fig. S3-(4). Note that when the determined number of y ranges is fewer than four, the identical y ranges are displayed multiple times.
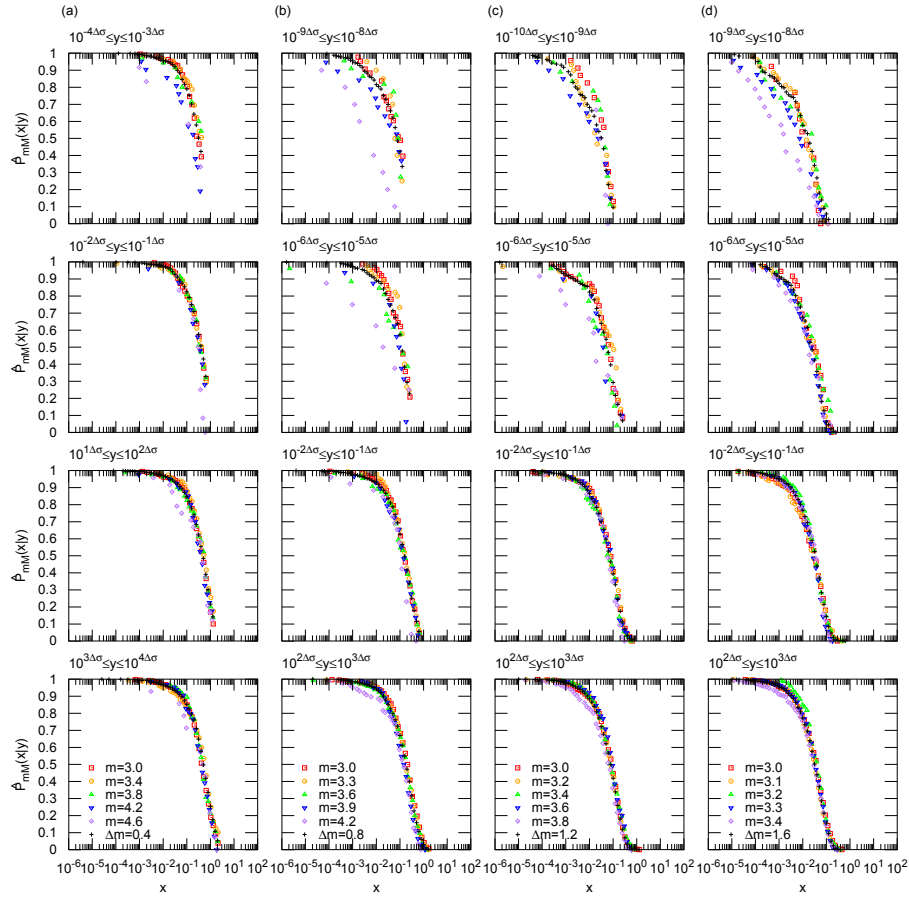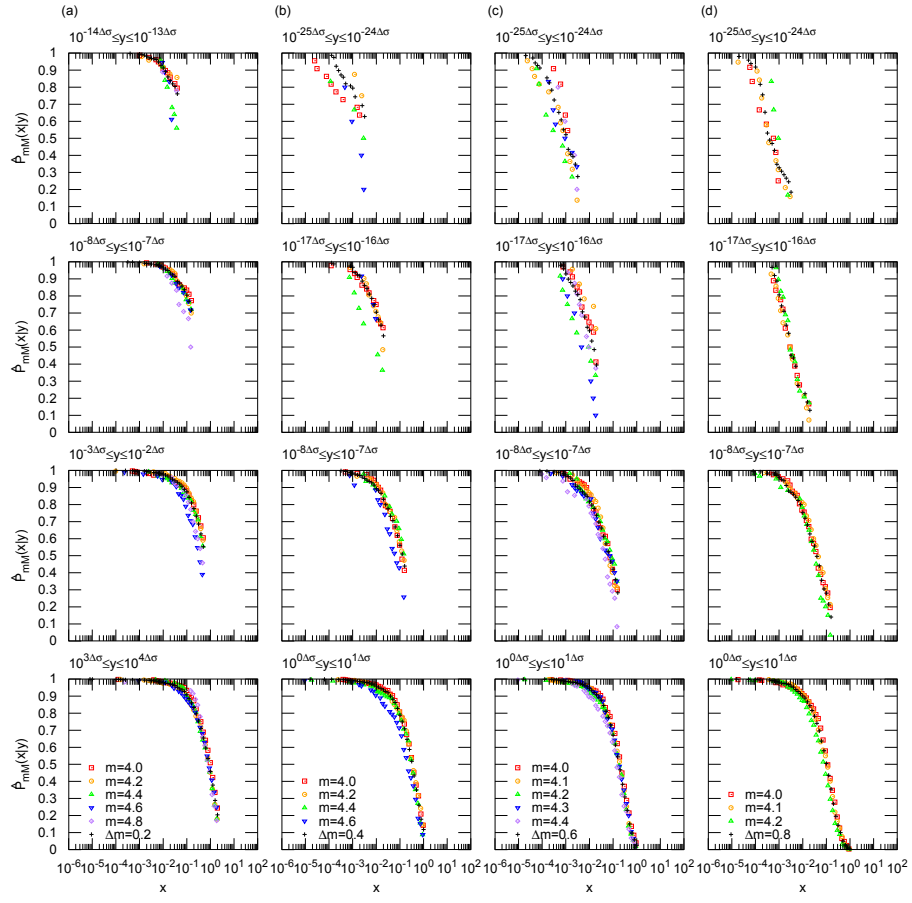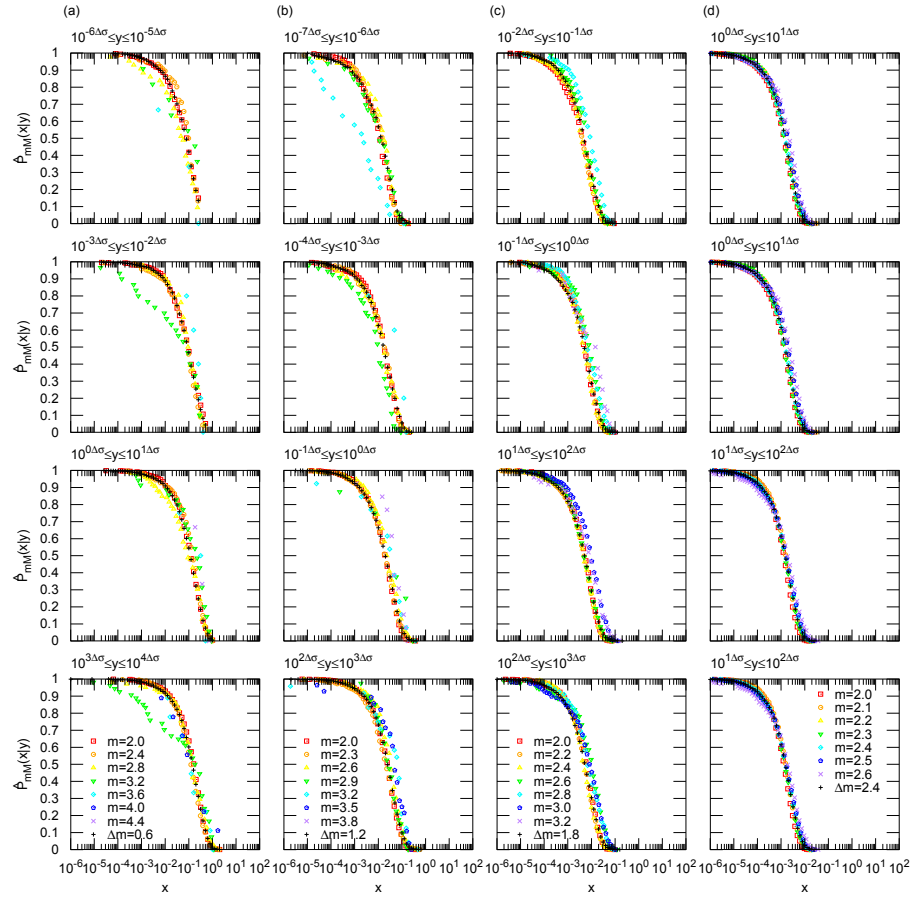

Figure S3-(1): JS
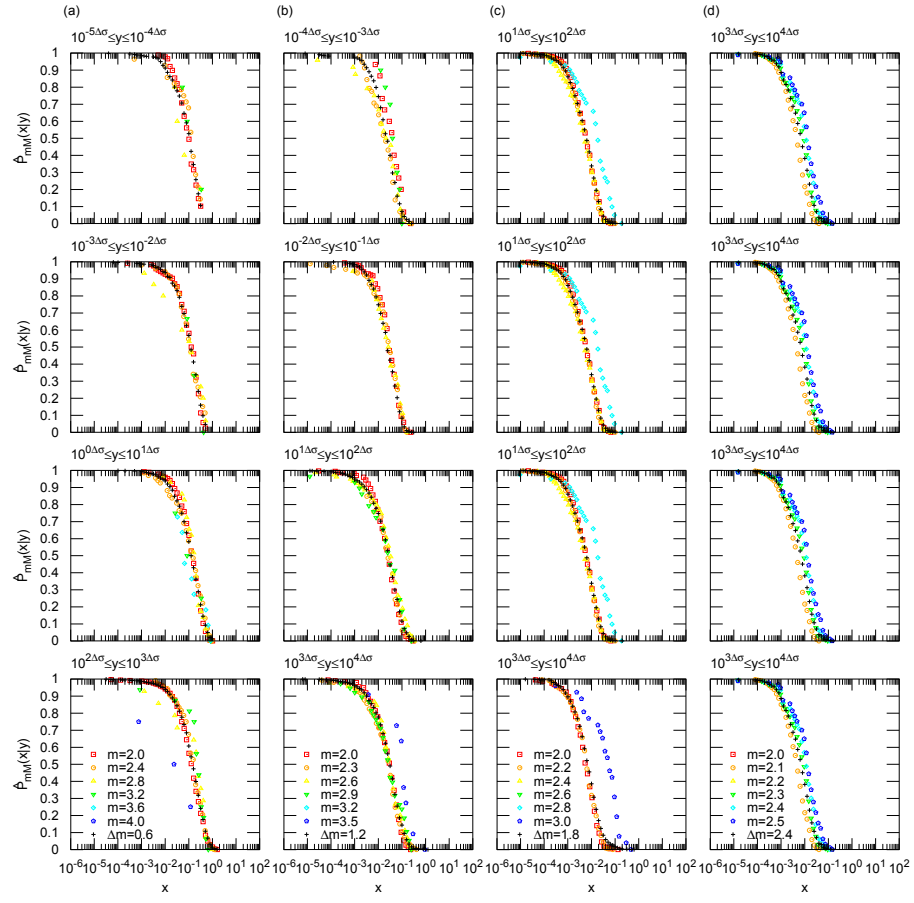
Figure S3-(2): JA
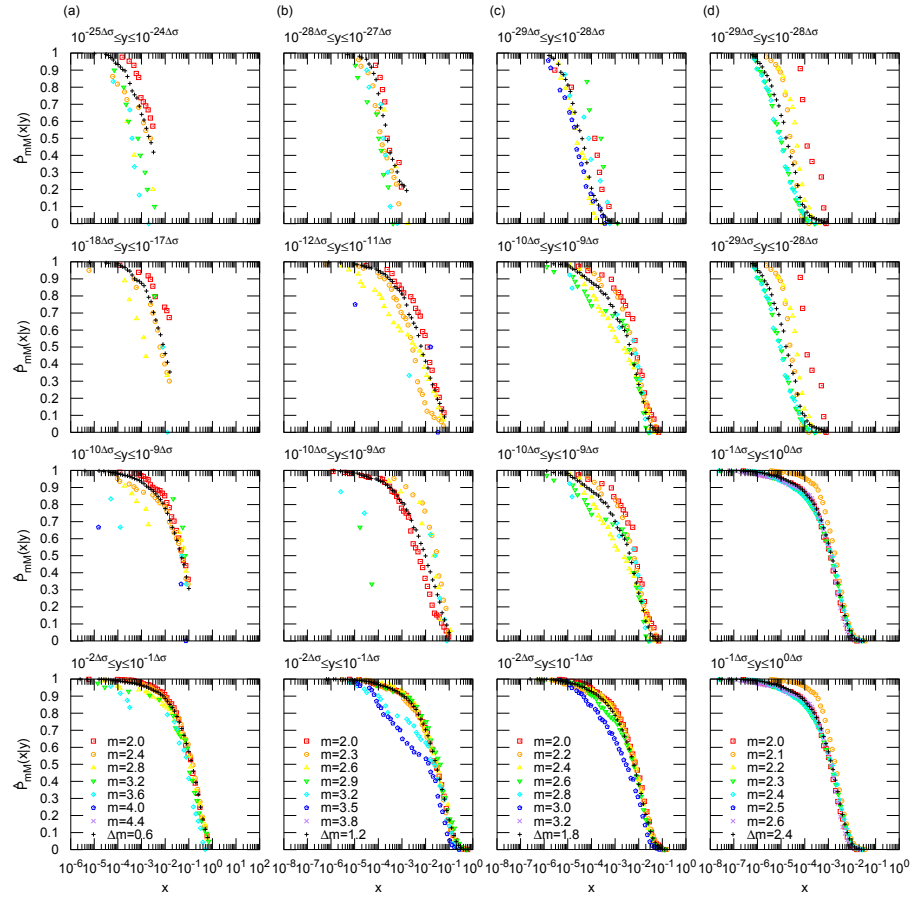
14

Figure S3-(3): SCA1
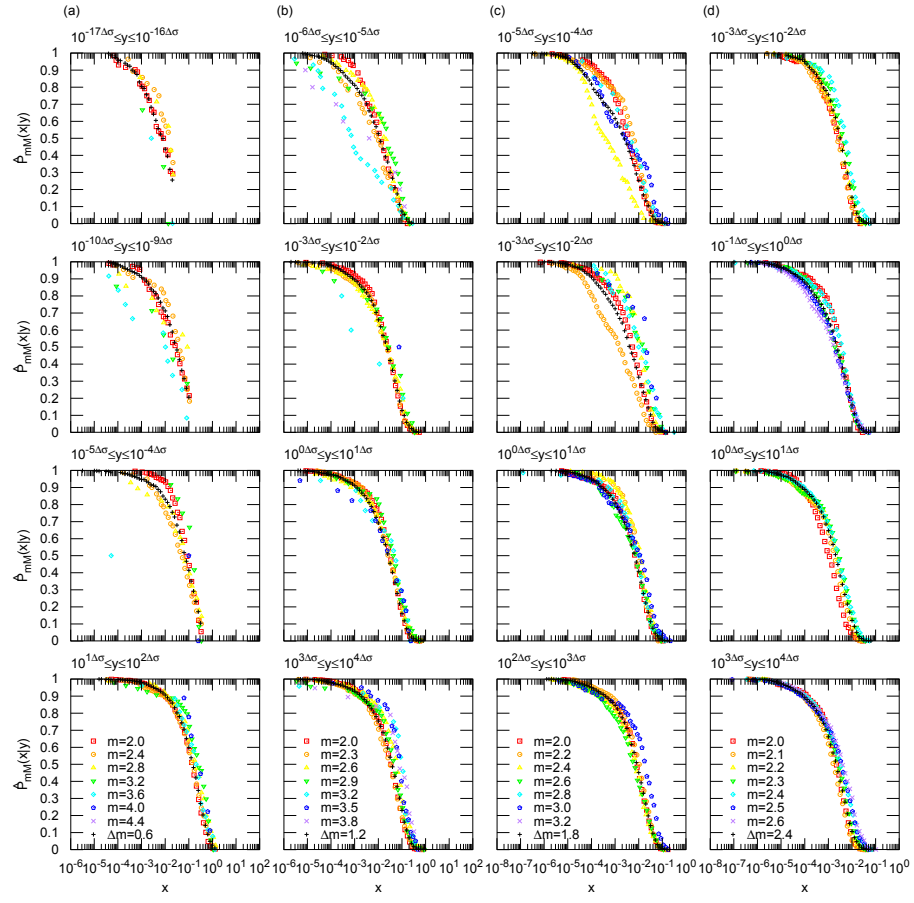
Figure S3-(4): SCA2

16

Figure S3-(5): SCA3
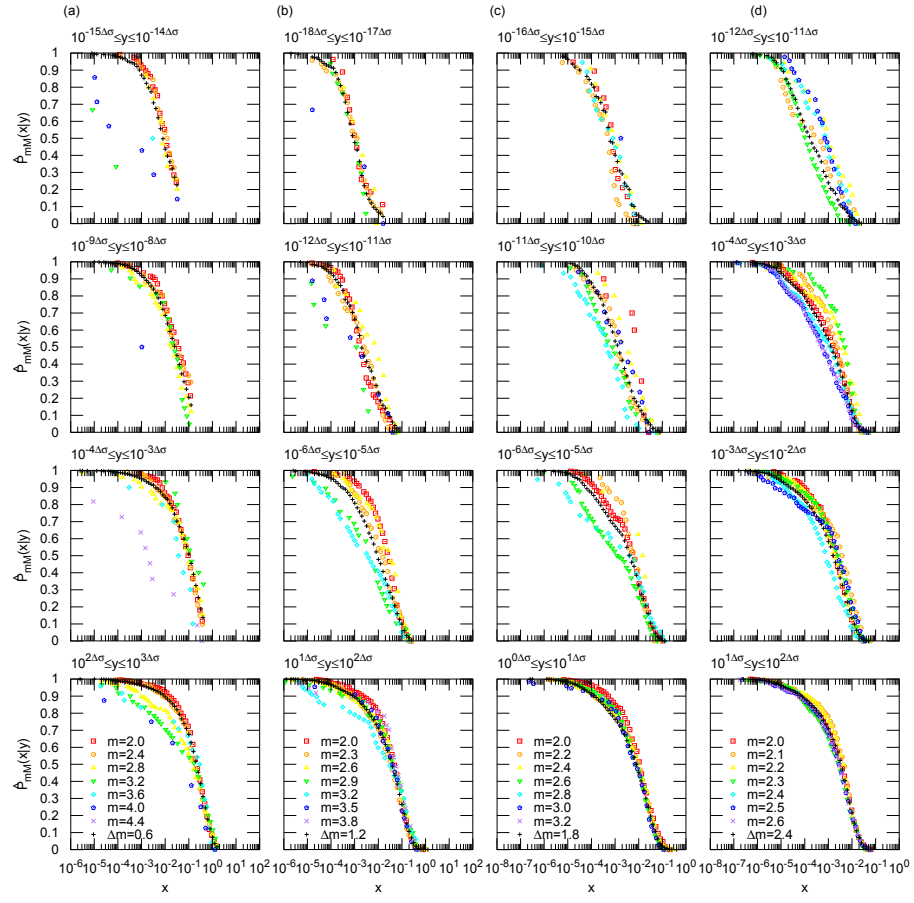
17

Figure S3-(6): SCS1

18

Figure S3-(7): SCS2

19

4 Figures S4- for $\hat{p}_{\Delta m}(x|y)$ and $\overline{p}_{\Delta m}(x|y)$

Figures S4-(1) to S4-(8) show $\hat{p}_{\Delta m}(x|y)$ and $\overline{p}_{\Delta m}(x|y)$ for each time series with:
(a) $\Delta m = 0.4$, (b) $\Delta m = 0.8$, (c) $\Delta m = 1.2$, and (d) $\Delta m = 1.6$ for S4-(1), S4-(2);
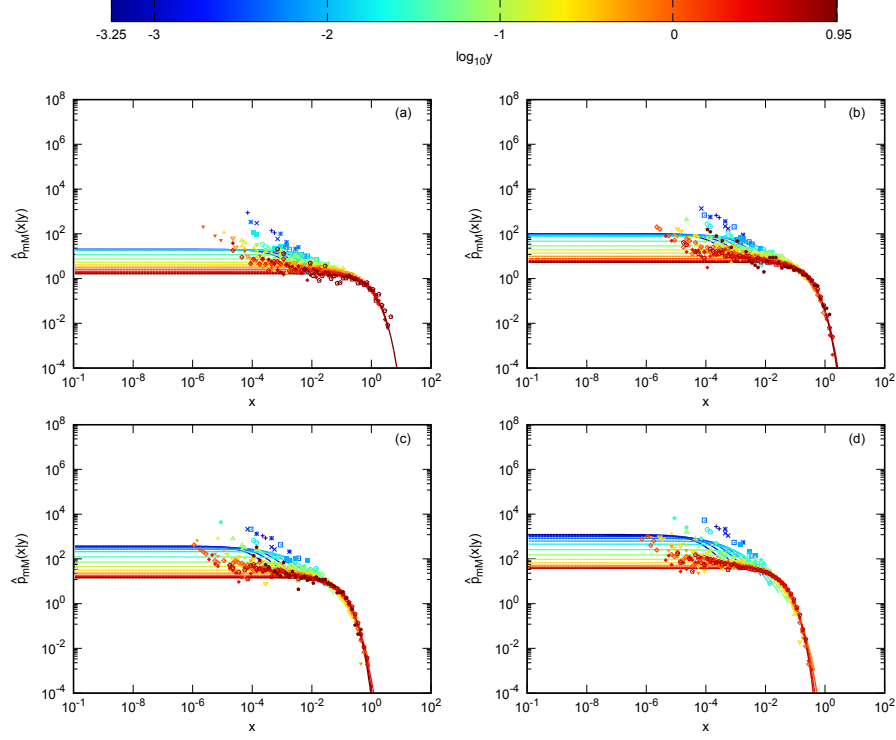(a) $\Delta m = 0.2$, (b) $\Delta m = 0.4$, (c) $\Delta m = 0.6$, and (d) $\Delta m = 0.8$ for S4-(3); (a)
$\Delta m = 0.6$, (b) $\Delta m = 1.2$, (c) $\Delta m = 1.8$, and (d) $\Delta m = 2.4$ for S4-(4) – S4-(8).
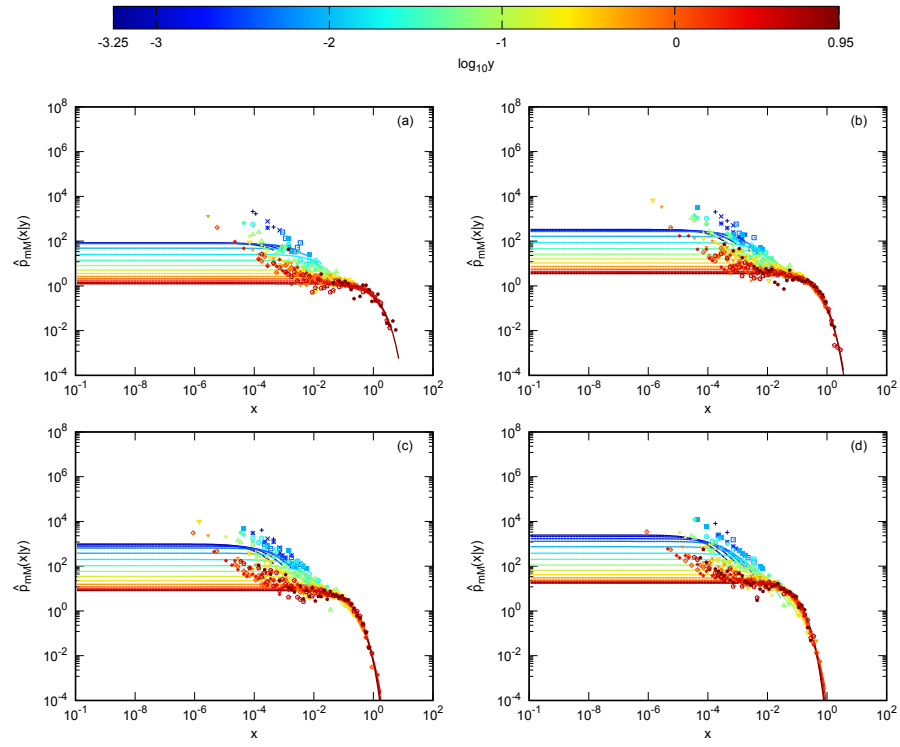

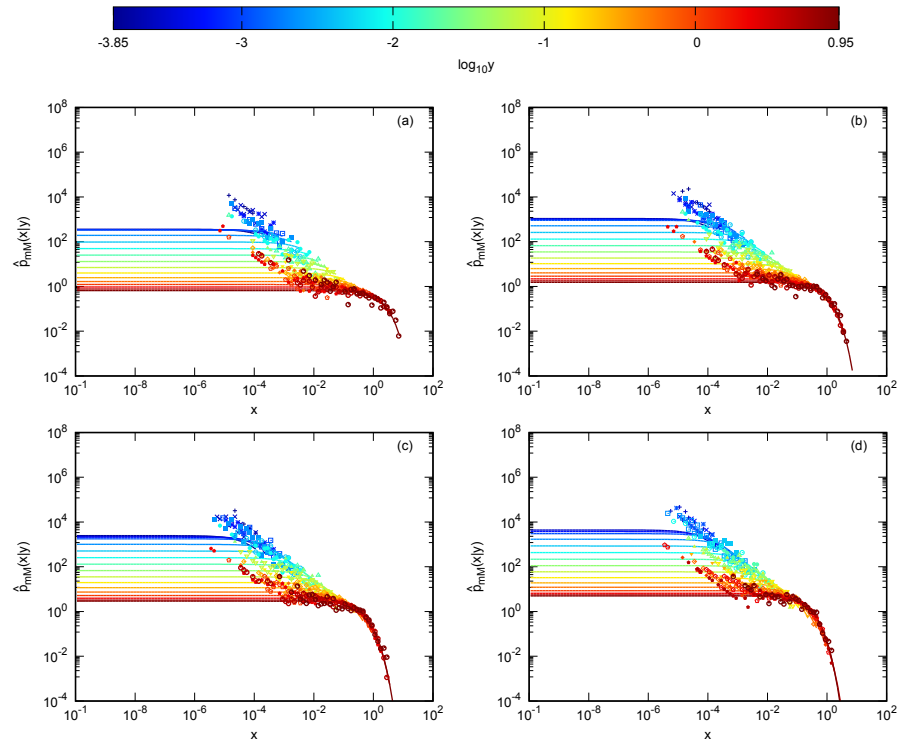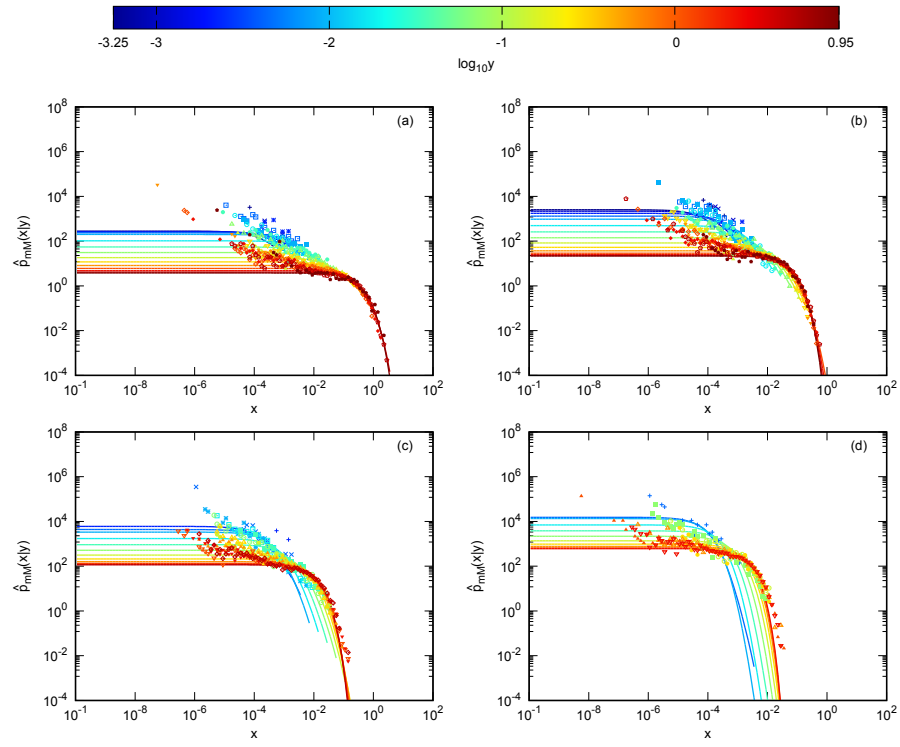Figure S4-(1): CMT

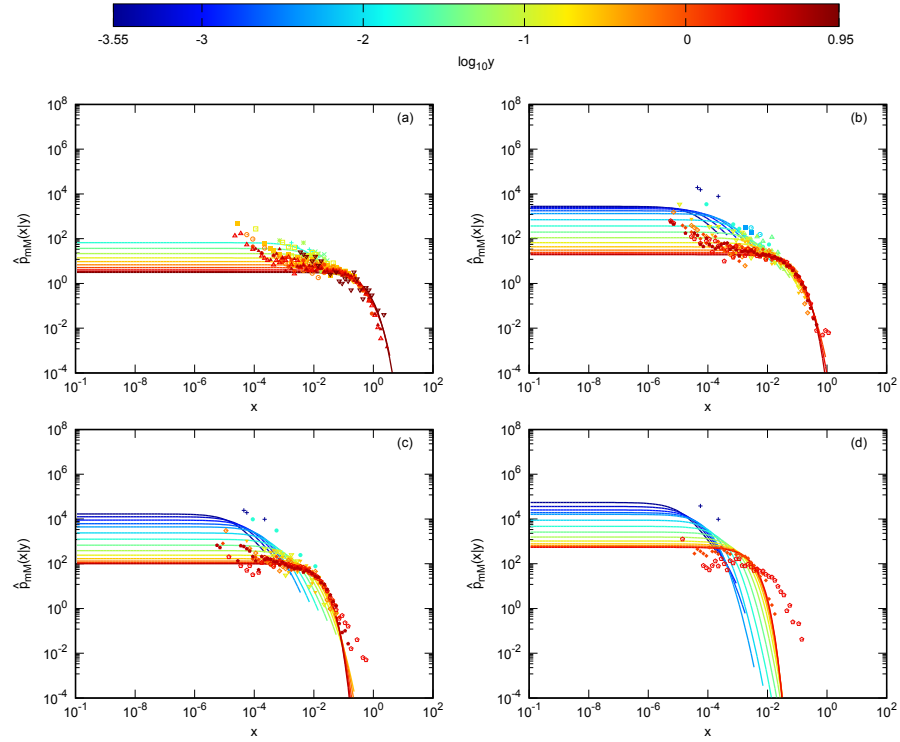Figure S4-(2): JS

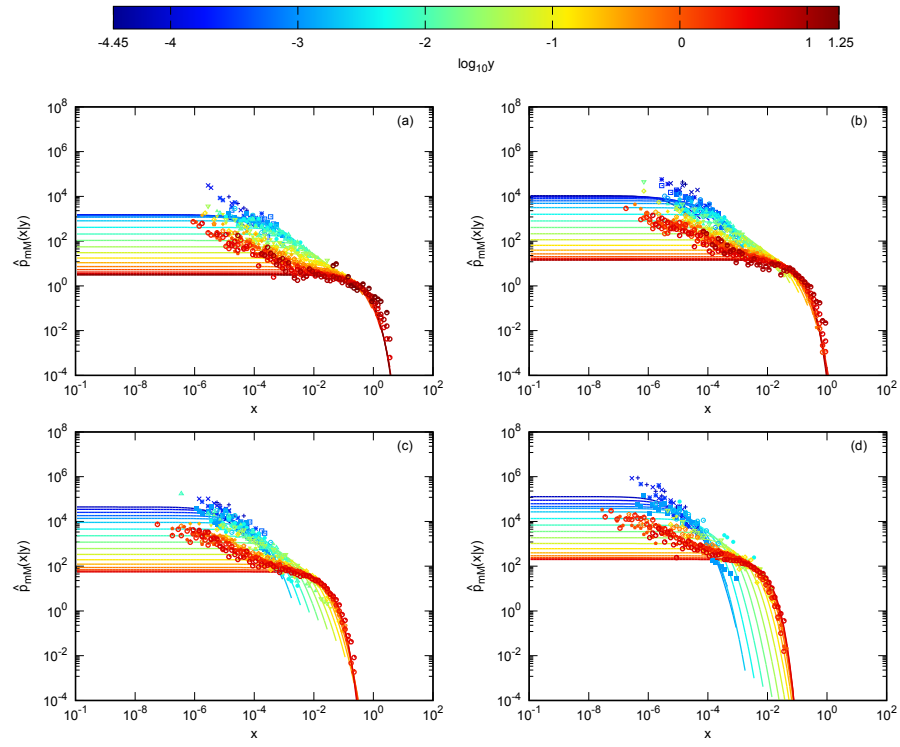Figure S4-(3): JA

Figure S4-(4): SCA1
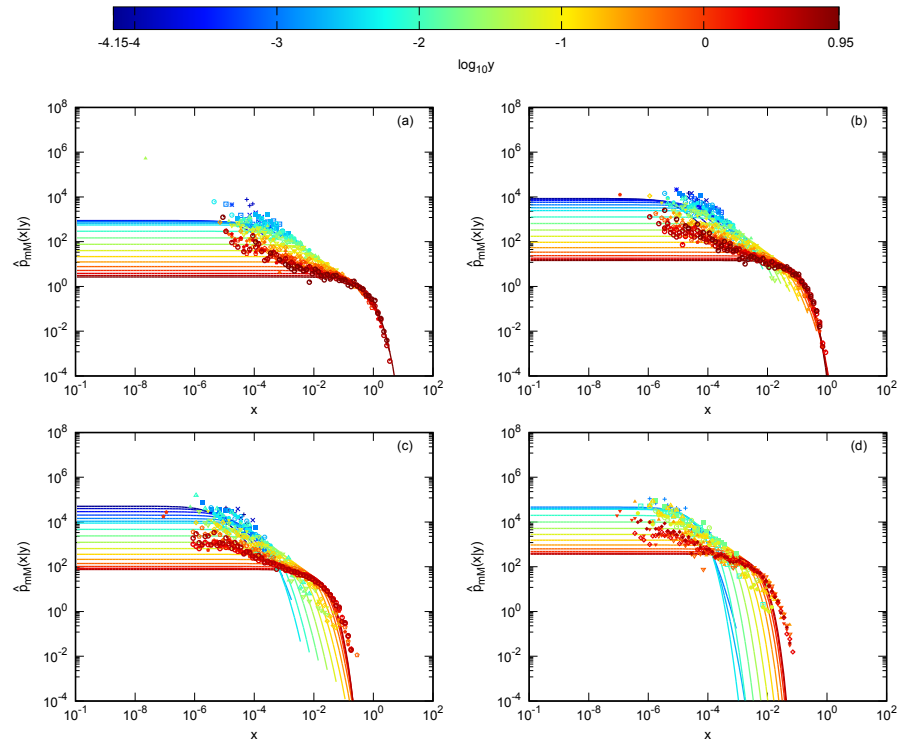

Figure S4-(5): SCA2

Figure S4-(6): SCA3
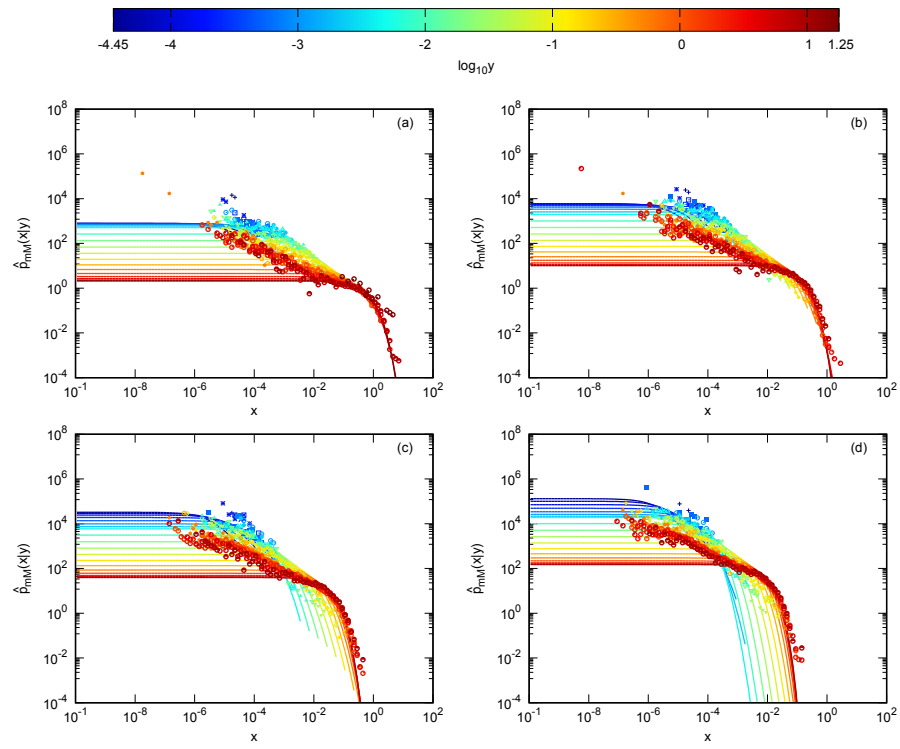

Figure S4-(7): SCS1

23

Figure S4-(8): SCS2

5 Figures S5- for $\hat{P}_{Mm}(y|x)$ and $\overline{P}_{\Delta m}(y|x)$

Figures S5-(1) to S5-(7) show $\hat{P}_{Mm}(y|x)$ and $\overline{P}_{\Delta m}(y|x)$ for each time series with: (a) $\Delta m = 0.4$, (b) $\Delta m = 0.8$, (c) $\Delta m = 1.2$, and (d) $\Delta m = 1.6$ for Fig. S5-(1); (a) $\Delta m = 0.2$, (b) $\Delta m = 0.4$, (c) $\Delta m = 0.6$, and (d) $\Delta m = 0.8$ for Fig. S5-(2); (a) $\Delta m = 0.6$, (b) $\Delta m = 1.2$, (c) $\Delta m = 1.8$, and (d) $\Delta m = 2.4$ for Figs. S5-(3) − S5-(7). The displayed y ranges in Fig. S5-(4) are chosen from such j' s that at least 5 of the (m, M)s indicated in the legend are in the range $(10^{j\Delta\sigma}, 10^{(j+1)\Delta\sigma})$. Note the same multi-times display of identical x ranges as in Fig. S3-.
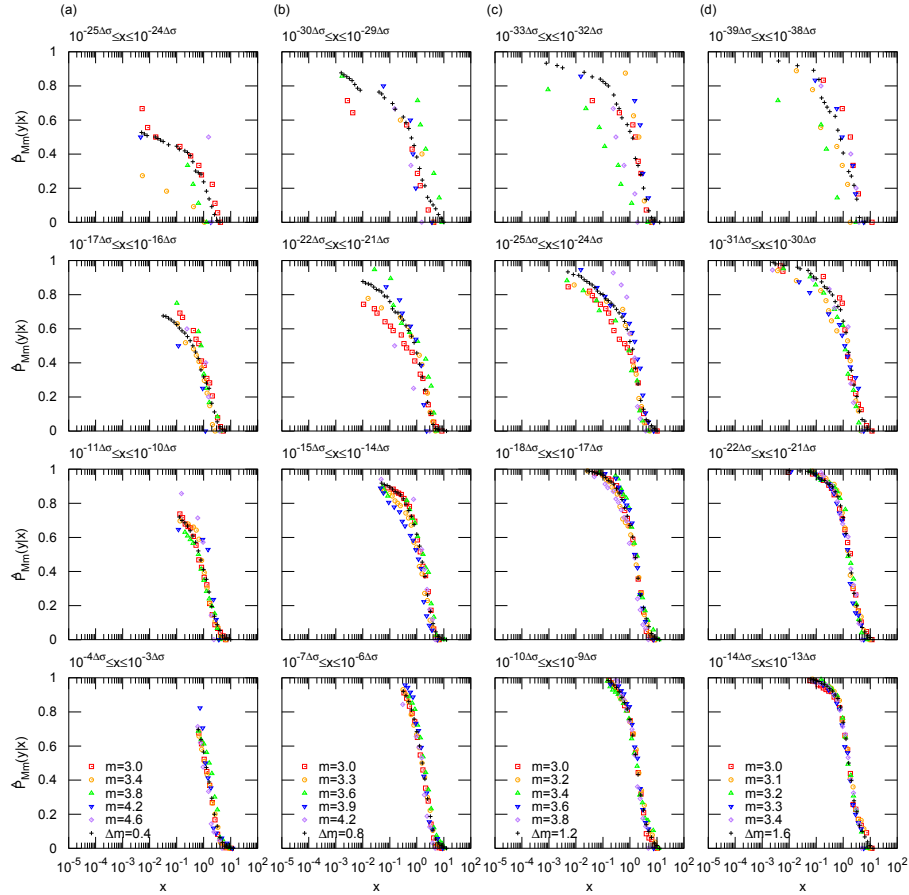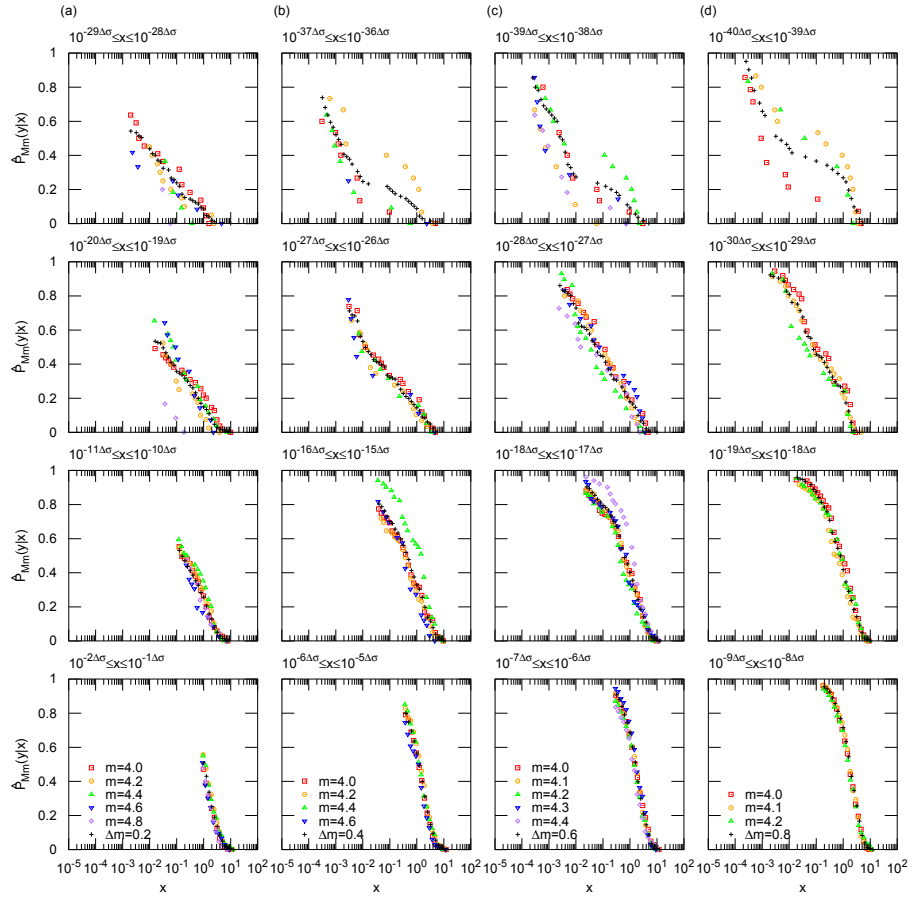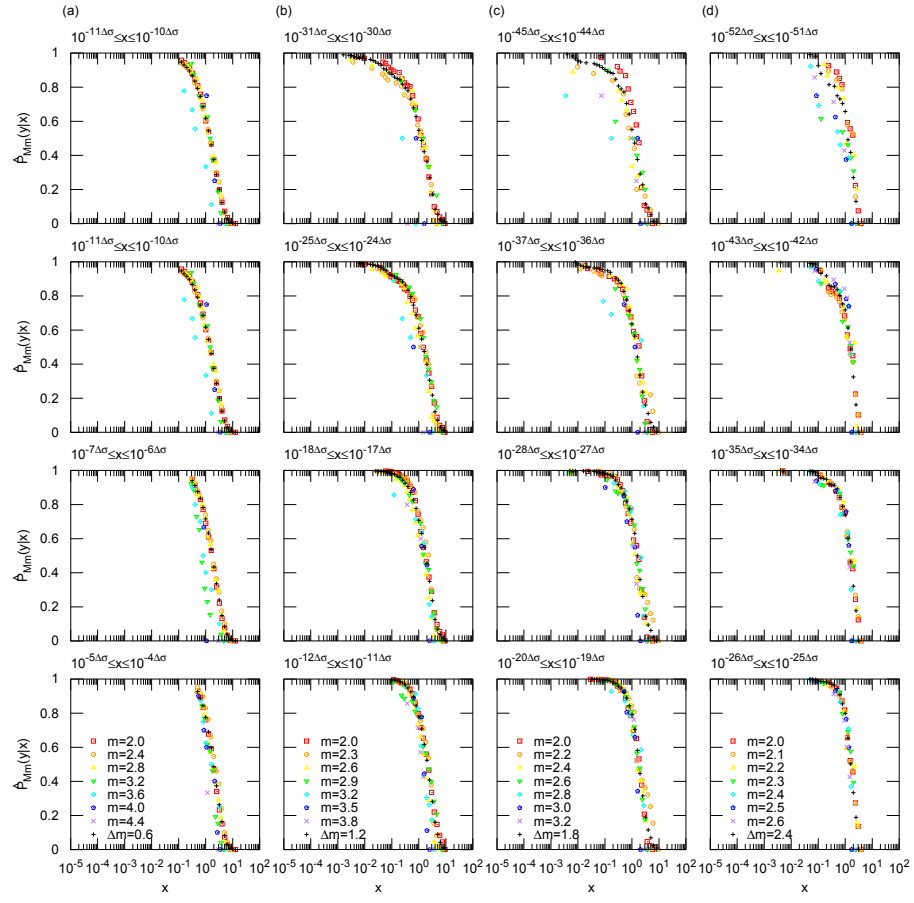

Figure S5-(1): JS
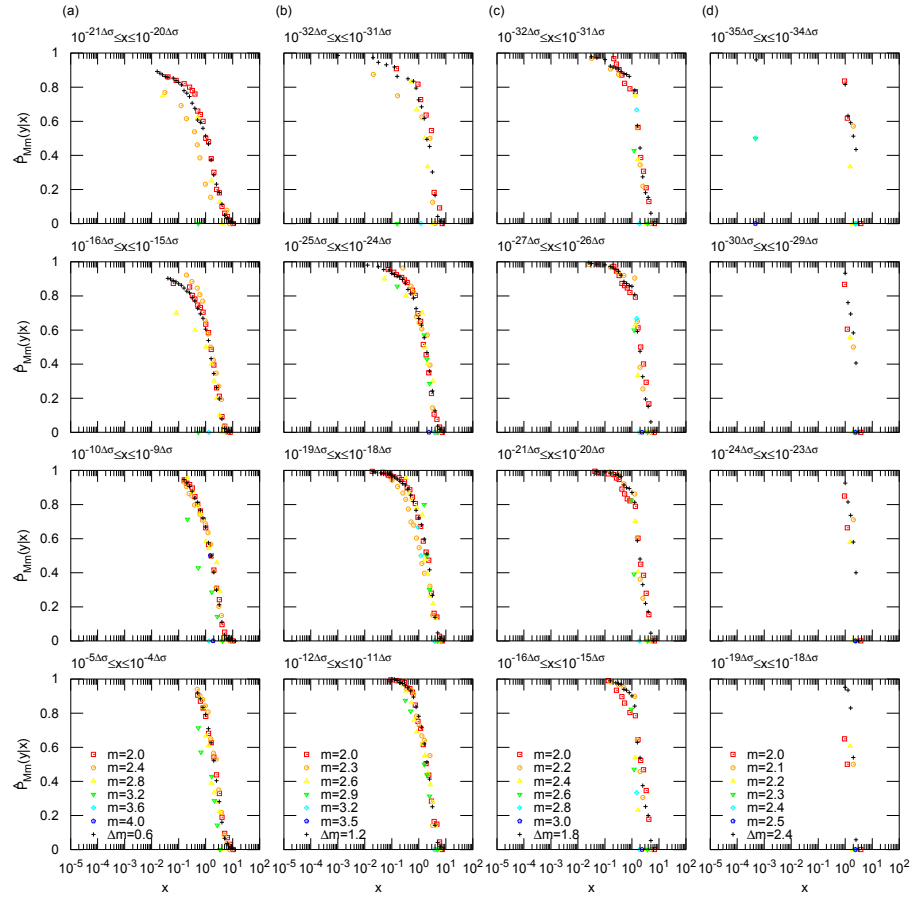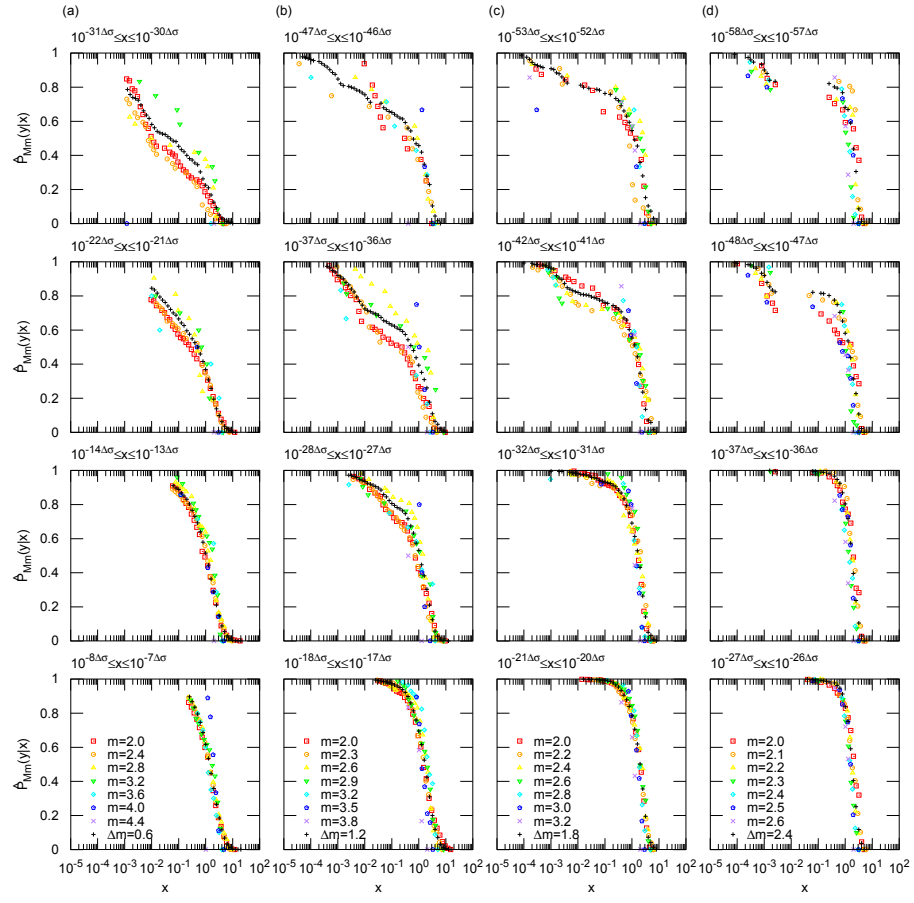
Figure S5-(2): JA

Figure S5-(3): SCA1

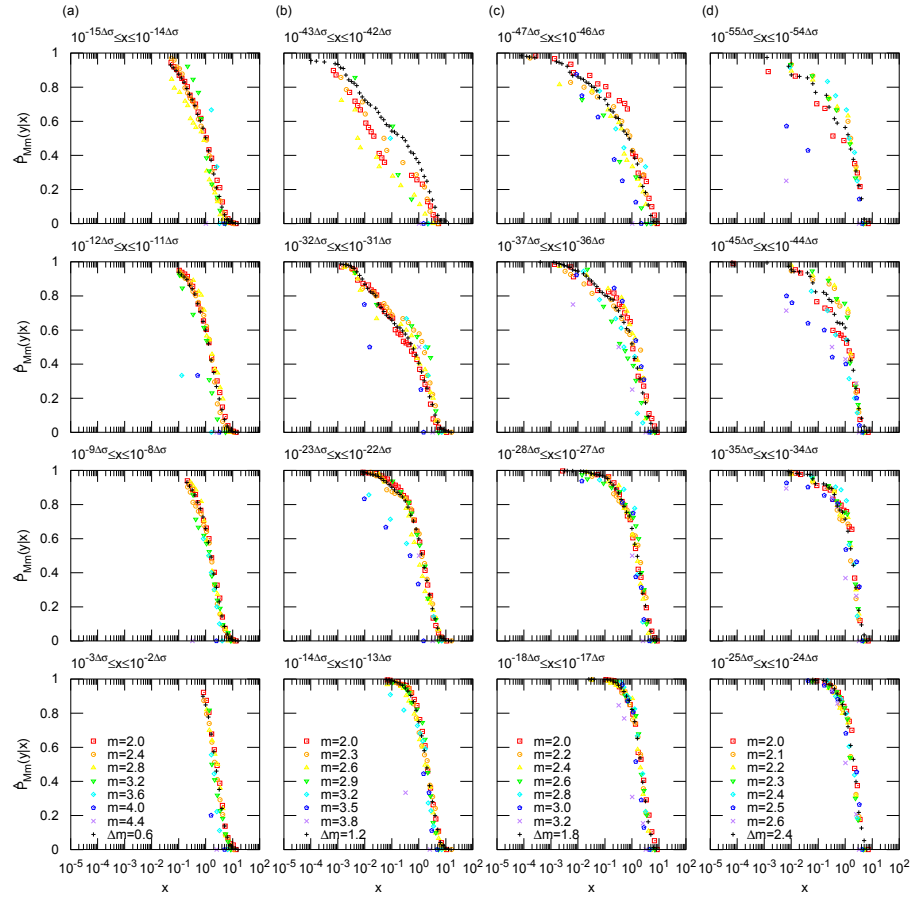Figure S5-(4): SCA2

28

Figure S5-(5): SCA3
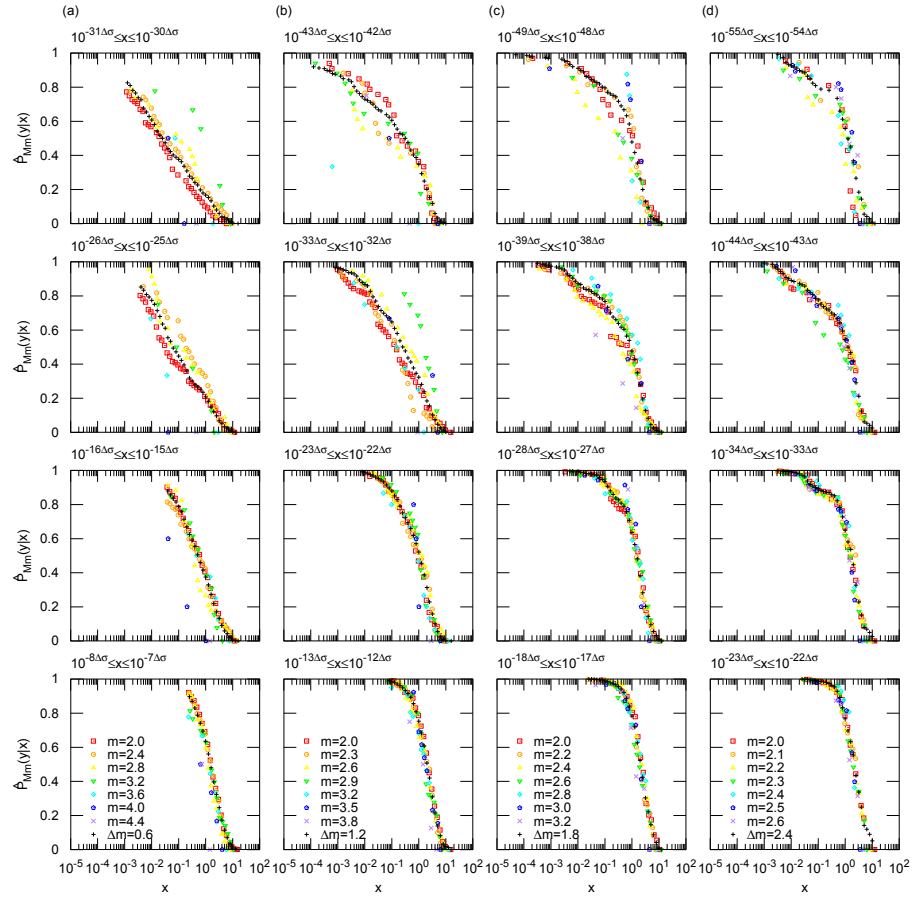
29

Figure S5-(6): SCS1

30

Figure S5-(7): SCS2

31

6   Figures S6- for $\hat{p}_{\Delta m}(y|x)$ and $\overline{p}_{\Delta m}(y|x)$

Figures S6-(1) to S6-(8) show $\hat{p}_{\Delta m}(y|x)$ and $\overline{p}_{\Delta m}(y|x)$ for each time series with Δm values: (a) Δm = 0.4, (b) Δm = 0.8, (c) Δm = 1.2, and (d) Δm = 1.6 for Figs. S6-(1), S6-(2); (a) Δm = 0.2, (b) Δm = 0.4, (c) Δm = 0.6, and (d) Δm = 0.8 for Fig. S6-(3); (a) Δm = 0.6, (b) Δm = 1.2, (c) Δm = 1.8, and (d) Δm = 2.4 for Figs. S6-(4) – S6-(8).
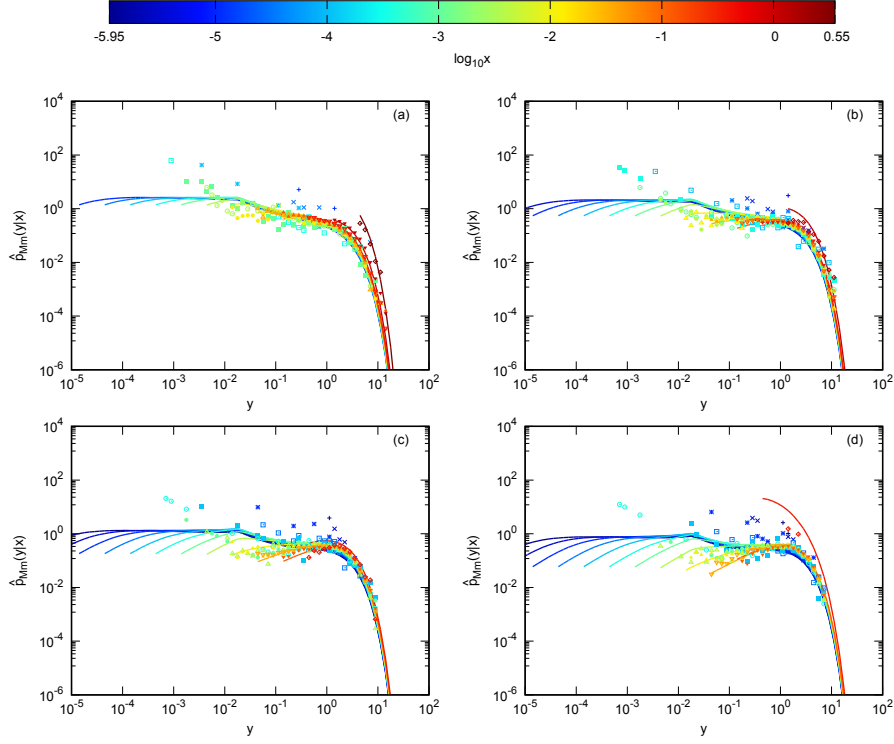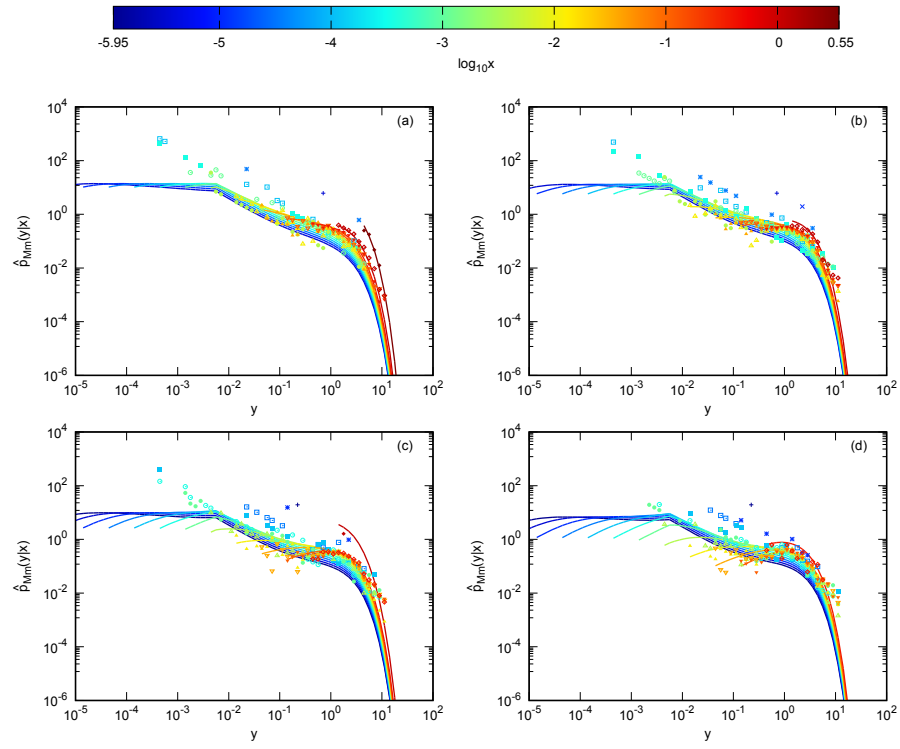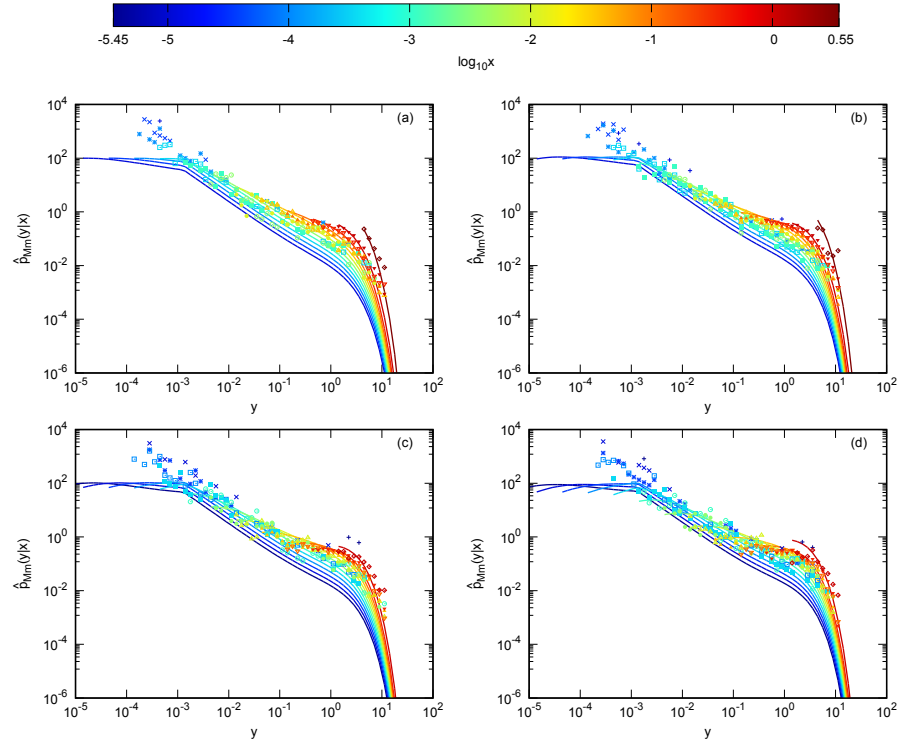

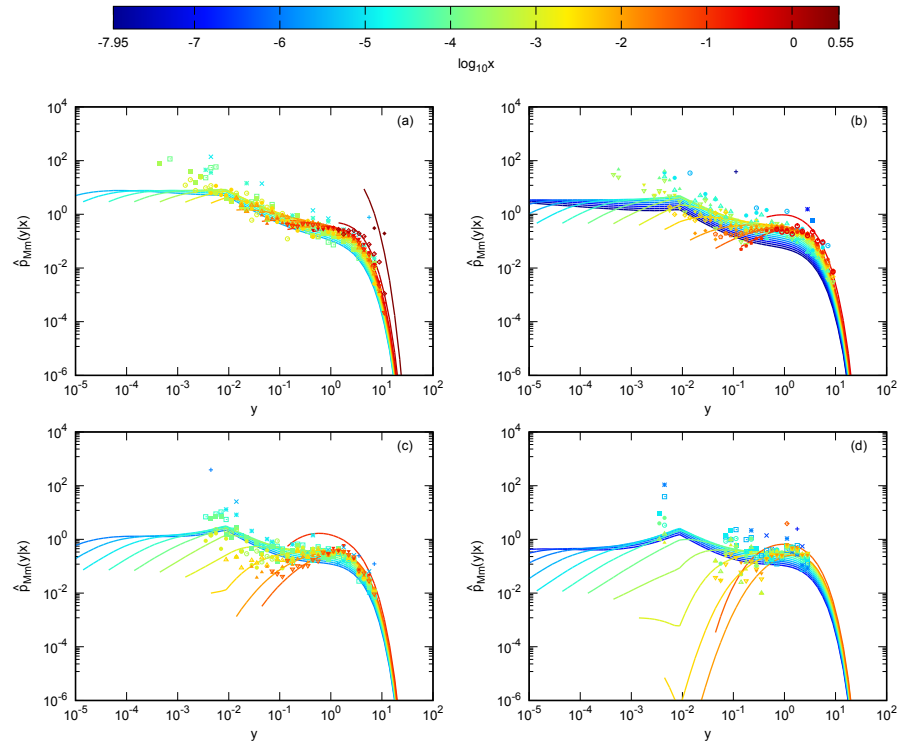
Figure S6-(1): CMT

Figure S6-(2): JS

Figure S6-(3): JA
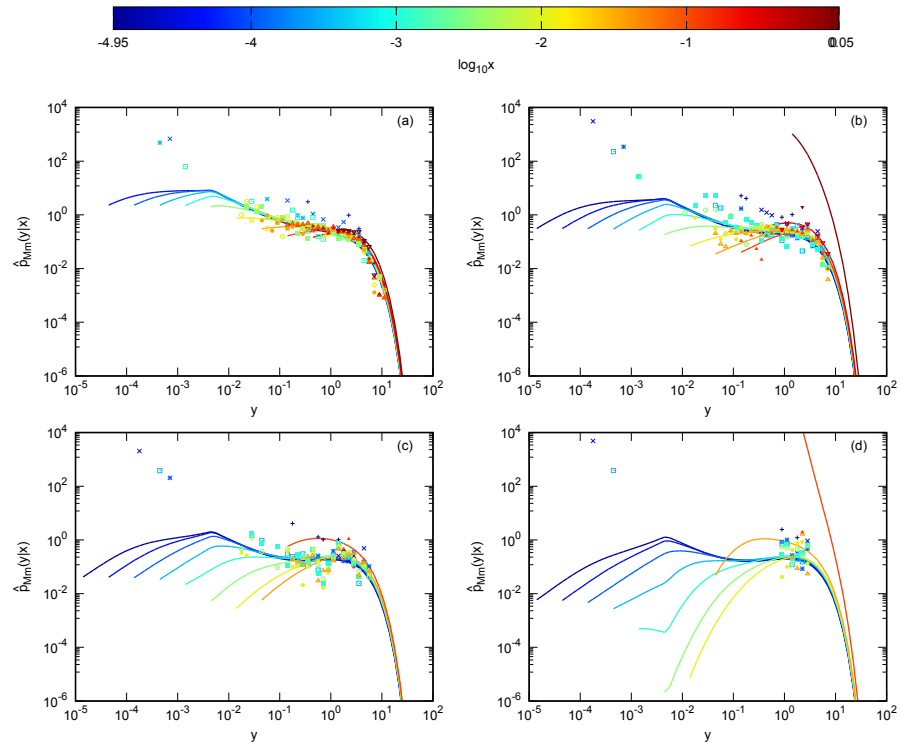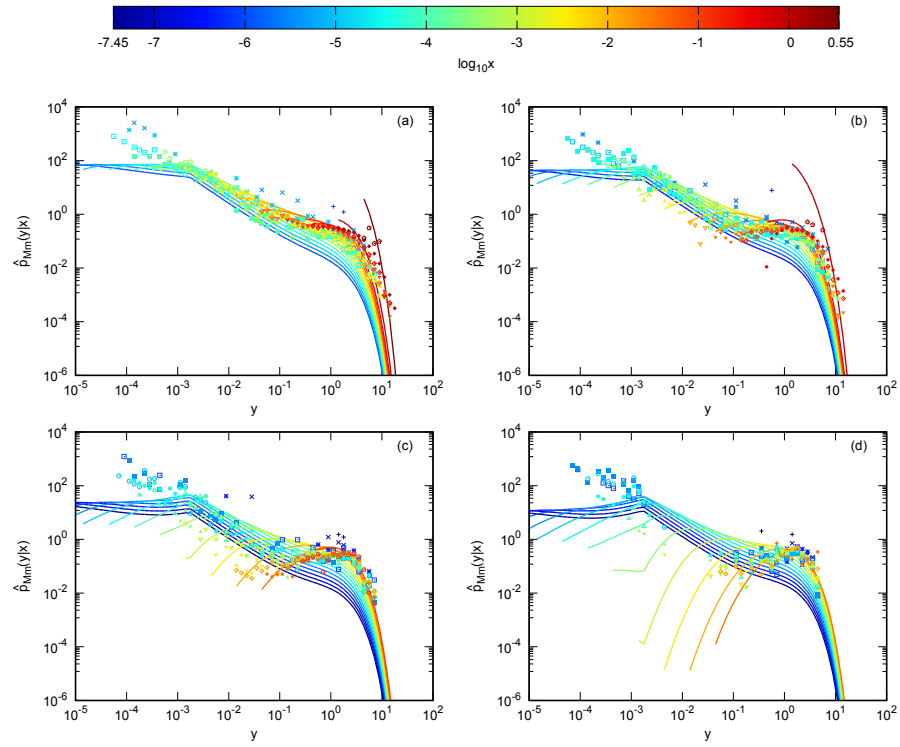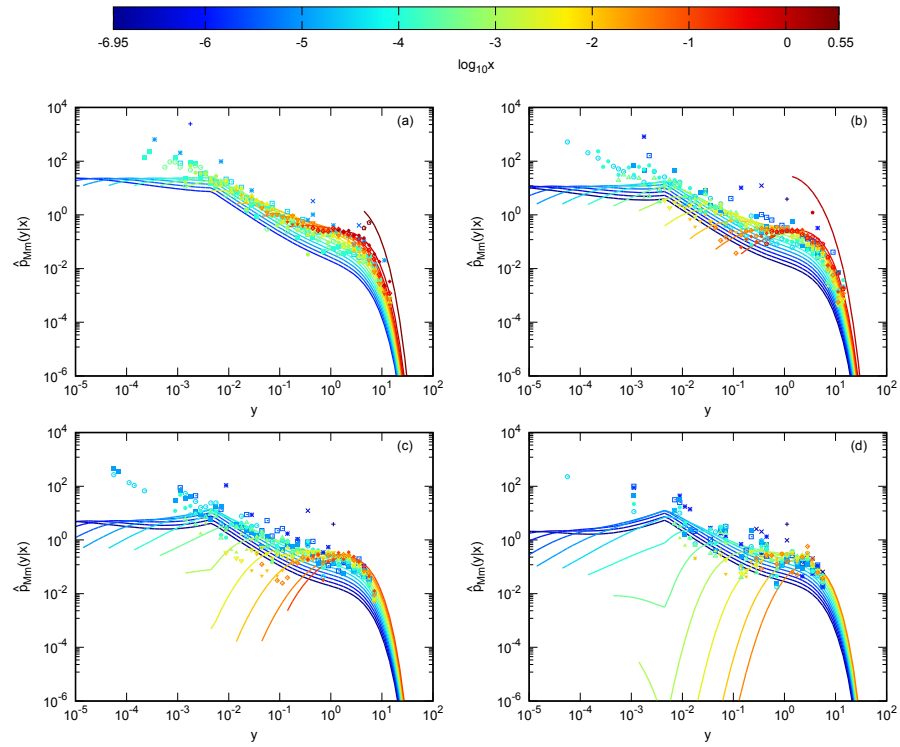
Figure S6-(4): SCA1

Figure S6-(5): SCA2

Figure S6-(6): SCA3

Figure S6-(7): SCS1

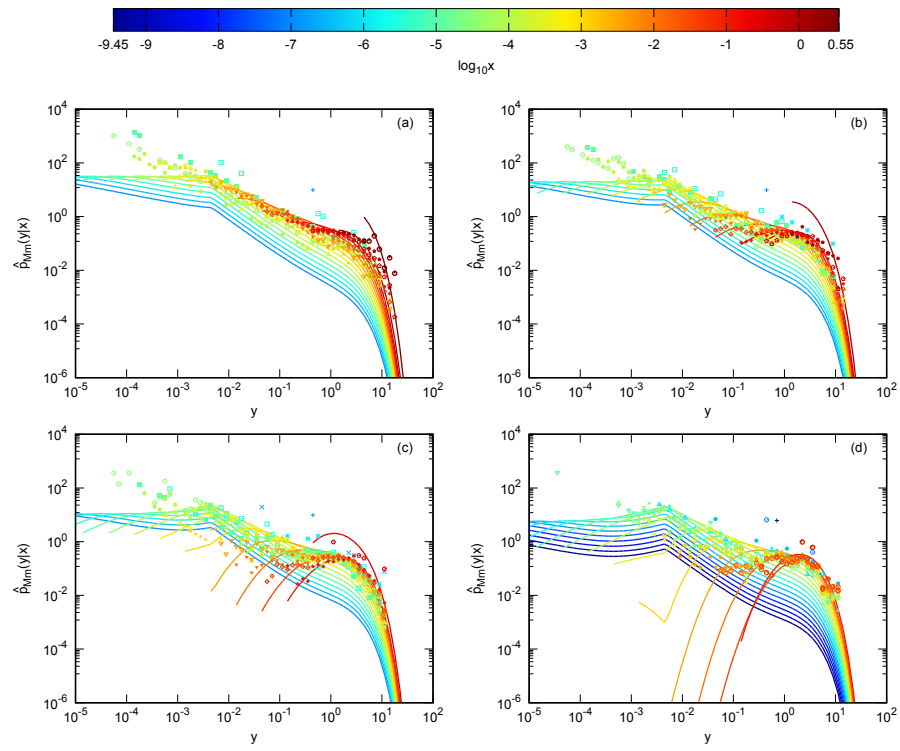Figure S6-(8): SCS2